

1 **The potential of reed canary grass and the importance of field**  
2 **heterogeneity for reducing GHG emissions in a rewetting fen**  
3 **peatland**

4 **Andres F. Rodriguez<sup>1</sup>, Johannes W.M. Pullens<sup>1,2</sup>, Jesper R. Christiansen<sup>3</sup>, Klaus S.**  
5 **Larsen<sup>3</sup>, and Poul E. Lærke<sup>1,2</sup>**

6 <sup>1</sup> Department of Agroecology, Aarhus University, Tjele, 8830, Denmark

7 <sup>2</sup> iCLIMATE Interdisciplinary Centre for Climate Change, Aarhus University, Roskilde,  
8 4000, Denmark

9 <sup>3</sup> Department of Geosciences and Natural Resource Management, University of Copenhagen,  
10 Copenhagen, 1958, Denmark

11

12 *Correspondence to:* Andres F. Rodriguez (afrodriguez@agro.au.dk)

## 13 Abstract

14 Rewetting drained peatlands can reduce CO<sub>2</sub> emissions but prevents traditional agriculture.  
15 Crop production under rewetted conditions may continue with flood-tolerant crops in  
16 paludiculture, but its effects on greenhouse gas (GHG) emissions compared to rewetting  
17 without further management are largely unknown. This study was conducted between 2021  
18 and 2022 on a fen peatland in central Denmark established with *Phalaris arundinacea* L.  
19 (Reed Canary Grass) in 2018. Three harvest/fertilization management treatments (0, 2, and 5-  
20 cut) were applied with the 2-cut and 5-cut treatments receiving 200 kg N ha<sup>-1</sup> y<sup>-1</sup> in equal split  
21 doses, whereas the 0-cut remained unfertilized. Measurements of CO<sub>2</sub> and CH<sub>4</sub> emissions  
22 were conducted biweekly under four different light intensities using a manual chamber  
23 connected to a gas analyzer. Although the mean annual water table depth (WTD) was -8 cm,  
24 indicating a rather wet peatland, the site remained a CO<sub>2</sub> source with a mean net ecosystem C  
25 balance (NECB) of 6.6 t C ha<sup>-1</sup> yr<sup>-1</sup> across treatments. Methane emissions averaged 90 kg of  
26 CH<sub>4</sub>-C ha<sup>-1</sup> yr<sup>-1</sup>, equivalent to 11.7% of NECB given as CO<sub>2</sub> equivalents. Results showed that  
27 management marginally increased biomass production reflected by more negative gross  
28 primary productivity (GPP) in 2-cut and 5-cut compared to 0-cut. No significant treatment  
29 effect was found on NECB due to field heterogeneity reflected by differences in pore water  
30 nutrient concentrations and WTD dynamics among the studied blocks, with higher R<sub>eco</sub>  
31 corresponding to blocks where higher pore water nutrient concentrations were observed. The  
32 results indicated that GHG emissions might potentially be reduced when the biomass is  
33 harvested from the more productive peatland area in comparison with no management,  
34 whereas on the less productive area it might be beneficial to leave the biomass unmanaged.  
35 Model simulation of ecosystem respiration (R<sub>eco</sub>) using WTD data of high temporal  
36 resolution captured the variability better as compared to the use of mean annual WTD, which  
37 underestimated R<sub>eco</sub> by 18% on average compared to the hourly WTD model. Data on pore

38 water chemistry further improved statistical linear models of CO<sub>2</sub> fluxes using soil  
39 temperature (Ts), WTD, ratio vegetation index (RVI) and photosynthetic active radiation  
40 (PAR) as explanatory variables. Overall, from a climate perspective the study supported  
41 biomass production compared to no management activity in rewetted fertile peatlands.

42

## 43 **1 Introduction**

44 Peatlands are an essential component of the global carbon (C) cycle. Covering only 3% of the  
45 terrestrial surface they store ~600 Gt of C, equivalent to 30% of the global soil C pool and  
46 exceeding the C stored in vegetation by ~150 Gt (Yu et al., 2010; Scharlemann et al., 2014;  
47 Erb et al., 2018; Leifeld and Menichetti, 2018). Northern temperate peatlands can be  
48 classified as bogs or fens and store 21.9 Gt C (Leifeld and Menichetti, 2018). While bogs are  
49 rain fed and nutrient poor, fens receive drain and ground water from the upland and  
50 occasionally from the streams under flooding conditions, making them minerotrophic with a  
51 pH close to neutral because the incoming waters carry minerals released from surrounding  
52 soils and sediments. Under high nutrient concentrations, fens are dominated by grasses and  
53 sedges such as *Phragmites* sp. and *Cladium* sp. (Page and Baird, 2016; Kreyling et al., 2021).

54 Peatland drainage creates aerobic conditions leading to peat mineralization, and consequently  
55 soil C is emitted as CO<sub>2</sub> to the atmosphere (Page and Baird, 2016), and dissolved C and  
56 nitrogen (N) compounds are leached from the soil (Cabezas et al., 2012; Liu et al., 2019).

57 Emissions from drained peatlands are estimated globally to 785 Mt CO<sub>2</sub> equivalents and the  
58 water table is considered the main controlling factor (Zhong et al., 2020; Evans et al., 2021)  
59 with higher water tables resulting in lower CO<sub>2</sub> emissions (Tiemeyer et al., 2020; Evans et al.,  
60 2021; Koch et al., 2023). However, other factors such as soil temperature (Ts), vegetation,  
61 and nutrient status may also affect CO<sub>2</sub> emissions from drained peat soils (Wilson et al.,

2016; Rigney et al., 2018; Bockermann et al., 2024). While rewetting reduces CO<sub>2</sub> emissions, it may also lead to increased CH<sub>4</sub> emissions (Wilson et al., 2016; Zhong et al., 2020; Darusman et al., 2023). The CO<sub>2</sub> / CH<sub>4</sub> emission trade-off depends on the water table, the origin of the water (bog/fen), type of vegetation (Rigney et al., 2018; Purre et al., 2019), its nutrient status (Wilson et al., 2016; Tiemeyer et al., 2020), as well as gradual changes in the microbial community following rewetting (Putkinen et al., 2018; Hemes et al., 2019; Emsens et al., 2020; Urbanova and Barta, 2020); However, even considering temporary increases in CH<sub>4</sub> emissions, peatland rewetting and restoration leads to the reestablishment of the C sink function of these ecosystems (Leifeld et al., 2019; Loisel and Gallego-Sala, 2022). Upon drainage, degradation of peat soils is manifested by increases in peat bulk density (Liu et al., 2019; Loisel and Gallego-Sala, 2022), and peat chemistry changes leading to decreasing C:N ratio, humic compounds, and polyphenols, while dissolved organic C (DOC) and N (DON) increase, these changes in peat chemistry may in turn enhance organic matter mineralization (Cabezas et al., 2012; Liu et al., 2019; Zak et al., 2019), and the release of nutrients along with higher bacterial and fungal activity increases CO<sub>2</sub> emissions (AminiTabrizi et al., 2022; Song et al., 2022).

78

The importance of peatlands for C storage and GHG emission mitigation, as well as other environmental services, has sparked an interest in peatland restoration with focus on rewetting (Page and Baird, 2016; Andersen et al., 2017). Rewetting can be achieved through different ways depending on the land use in the peatland after raising the water table. Peatlands have often been rewetted without altering the already established plant community or with the attempt to reestablish the native plant community. Paludiculture has been suggested as an alternative land use, enabling continued agricultural biomass production on

86 the rewetted peatlands under low or high management intensity (Tanneberger et al., 2020;  
87 Ziegler, 2020). Paludiculture is expected to reduce CO<sub>2</sub> emissions due to the water-saturated  
88 conditions of the peat soils (Ren et al., 2019; Tanneberger et al., 2020; De Jong et al., 2021)  
89 while producing biomass for renewable energy such as biogas production (Dragoni et al.,  
90 2017; Ren et al., 2019; Hartung et al., 2020) or insulation material that can be used as a green  
91 alternative in the building industry (De Jong et al., 2021). Paludiculture may also have the  
92 potential to remove excess nutrients from rewetted peatlands by nutrient removal with the  
93 harvested biomass (Giannini et al., 2017; Vroom et al., 2018; Geurts et al., 2020).

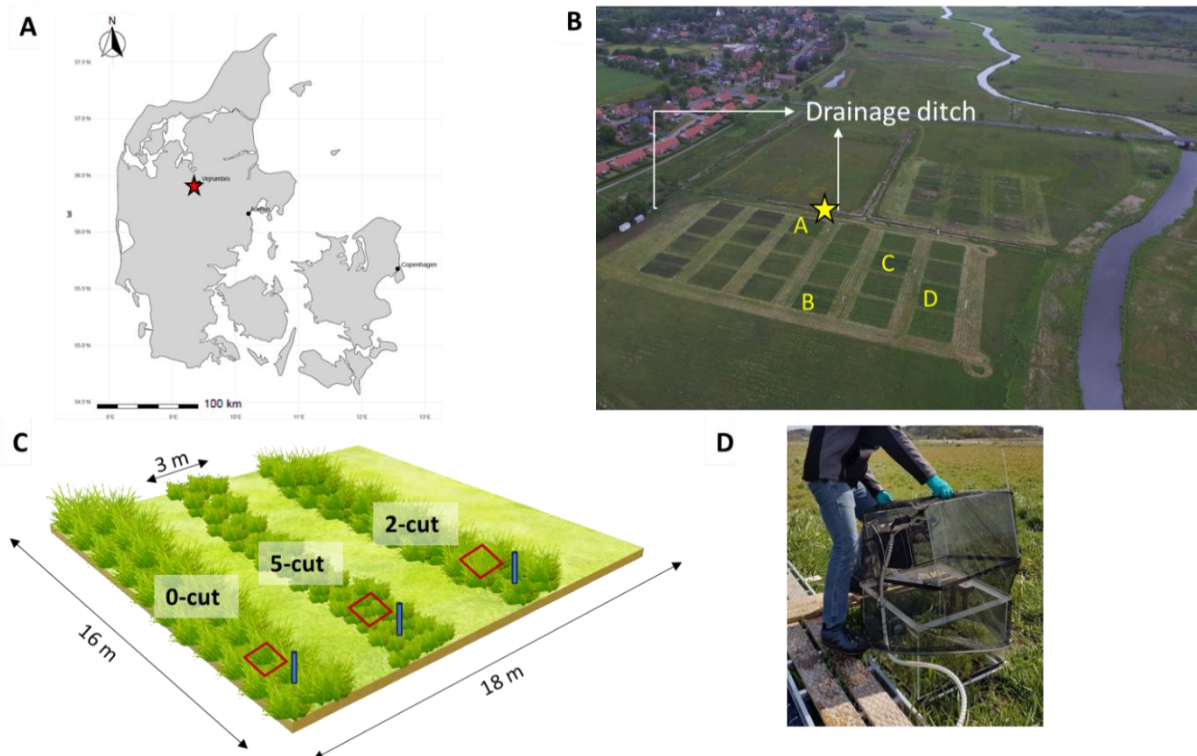
94 Large variation in quantified annual GHG emission from different land use of rewetted  
95 peatlands including paludiculture have been reported and further studies are needed to  
96 establish emission factors accordingly (Bianchi et al., 2021). It is well accepted that GHGs  
97 from rewetted peatlands are influenced by their nutrient content and water table level,  
98 reflected by IPCC Tier 1 emissions factors (Wilson et al., 2016). Mean annual water table  
99 depth has also been used to predict the net ecosystem carbon balance (NECB), but much  
100 uncertainty remains (Tiemeyer et al., 2020; Evans et al., 2021; Koch et al., 2023). The  
101 complexity and temporal resolution of gap filling models can also influence the NECB  
102 estimates (Karki et al., 2019; Liu et al., 2022) and it is highly uncertain how different  
103 management practices, water table dynamics during the year, and nutrient status affect annual  
104 emission budgets. Consequently, the objectives of this study were to: (1) determine the  
105 NECB of *Phalaris arundinacea* L. (reed canary grass; RCG) production under three harvest  
106 and fertilization management regimes during the third year after establishment in a fen  
107 peatland with shallow WTD, (2) assess model performances in gap filling biweekly  
108 measurements of ecosystem respiration ( $R_{\text{eco}}$ ) and gross primary productivity (GPP), and (3)  
109 investigate the relation of soil water chemistry with  $R_{\text{eco}}$  and GPP. We hypothesized that, (a)  
110 fertilization and harvest of RCG would increase C emissions compared to no RCG

111 management, (b) use of high-temporal frequency data on water table depth (WTD) would  
112 improve model prediction of ecosystem respiration ( $R_{eco}$ ), and (c) knowledge on soil pore  
113 water chemistry would improve explanation of C fluxes.

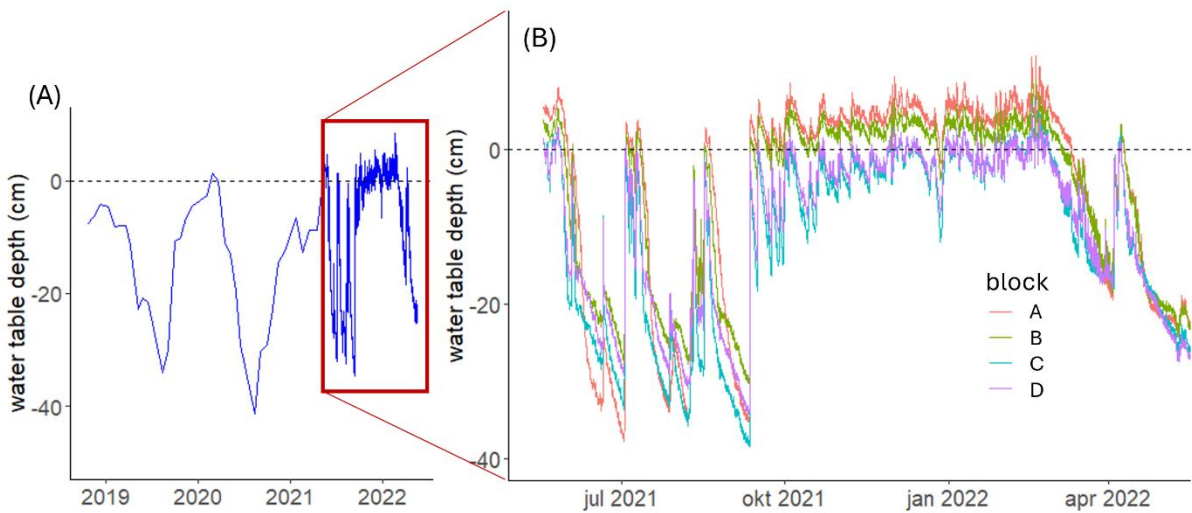
## 114 **2 Materials and methods**

### 115 **2.1 Study area**

116 This study was conducted from May 2021 to May 2022 at a riparian fen peatland located in  
117 the Nørreå valley, Vejrumbro, Central Jutland, Denmark (56°26'15.3''N, 9°32'44.1''E) (Fig  
118 1). The site was drained in the 1930s and used for agriculture predominantly under grassland  
119 rotation and grazing. The field became gradually wetter because of land subsidence, and the  
120 water level was largely controlled by the Nørreå stream, located at the southern border of the  
121 peatland (Malinowski et al., 2015). After 2018, maintenance of the drainage ditches stopped  
122 and the mean annual WTD gradually increased during the following years reaching -8 cm  
123 during the study year (18 May 2021 to 17 May 2022), with a minimum of -35 cm in the  
124 summer and a maximum of 8 cm in the winter across the experimental blocks (Fig 2a). The  
125 mean air temperature and total precipitation during the study year, measured at the  
126 Foulumgard meteorological station (Danish Meteorological Institute), located 6 km from the  
127 study site, were 9 °C and 709 mm, respectively. The peat layer at the study site has an  
128 average depth of 2 m, covering up to 10 m of gyttja (Mashadi et al., 2024). The  
129 physicochemical characteristics of the peat at the study area were measured for the top 1  
130 meter of the soil as part of a previous study by Nielsen et al. (2023b). Table 1 shows the peat  
131 characteristics for the four studied blocks.



132  
 133 Figure 1. A, map of Denmark, red star indicates the study site location; B, aerial photograph  
 134 of study site, letters indicate the four studied blocks, and yellow star indicates where the ditch  
 135 water samples were taken from; C, diagram of one of the blocks showing the three  
 136 randomized harvest treatment plots (0-cut, 2-cut, and 5-cut) and the location of collars (red  
 137 squares) and piezometers (blue cylinders); D, transparent chamber with shroud used for gas  
 138 measurements.



139  
 140 Figure 2. Panel (A) presents water table depth (WTD) across the experimental blocks as  
 141 measured in each block with intervals of 2-3 weeks at the study site from October 2018 to  
 142 April 2021 and every hour from May 2021 until May 2022 (red square). Panel (B) presents  
 143 the hourly WTD shown in the red square as the mean of each block with different colors.

144 Table 1. Soil physicochemical characteristics across 0-100 cm depth in the four studied  
 145 blocks (A-D).

Block	OM	pH	pb	TC	TN	C:N
	%		g cm <sup>-3</sup>	g kg <sup>-1</sup>	g kg <sup>-1</sup>	
A	85	5.6	0.15	440	26	17
B	83	6.0	0.15	430	28	14
C	70	6.2	0.18	374	24	15
D	75	6.2	0.13	401	27	15
Mean	78	6.0	0.15	411	26	15

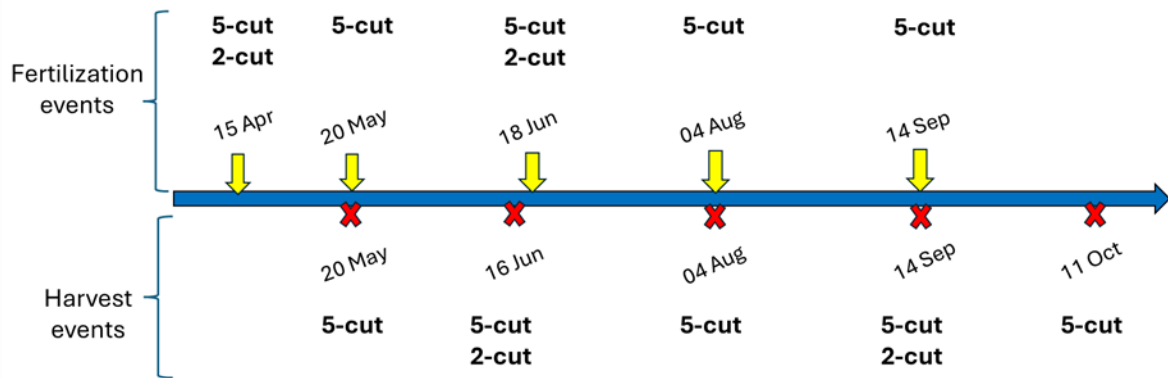
147 †OM, organic matter; pb, bulk density; TC, total C; TN, total N; C:N, carbon to nitrogen  
 148 ratio.

149

## 150 2.2 Experimental design

151 Four blocks (indicated by A, B, C and D on Fig 1B) were established with RCG, cultivar  
 152 Lipaula in 2018 as part of a larger field experiment. Each block had six randomly placed  
 153 plots with six different harvest and fertilization treatments whereof only three (0-cut, 2-cut, 5-  
 154 cut; referring to the number of harvest events applied) were used for this study. Thus, the  
 155 experimental design of this study, which is the same as Nielsen et al. (2024), consists of four  
 156 replicate blocks, each with three harvest/fertilization treatments. Harvest and fertilization  
 157 dates are shown in Figure 3. The harvested plots were fertilized with 200 kg N ha<sup>-1</sup> and 178  
 158 kg K ha<sup>-1</sup> in total, given as NPK 18-0-16 in equal split doses. Thus, the 2-cut and the 5-cut  
 159 received 100 kg N ha<sup>-1</sup> and 40 kg N ha<sup>-1</sup> for each cut, respectively, while the 0-cut did not  
 160 receive any fertilizer. The dimensions of the blocks and plots were (16 x 18 m), and (16 x 3  
 161 m), respectively (Fig 1C). Further details of the experimental design can be found in Nielsen  
 162 et al. (2021). At each plot, one 55 x 55 cm collar was installed to 10 cm depth to facilitate  
 163 closed, non-steady-state chamber measurements of net CO<sub>2</sub> and CH<sub>4</sub> fluxes. A piezometer  
 164 with a screen from 5 cm to 100 cm soil depth was installed 10-20 cm away from the collar at  
 165 each plot for soil water sampling. Ts at 5 cm soil depth and WTD were measured  
 166 continuously at hourly intervals using Ts dataloggers (HOBO Pendant temperature/light 64K  
 167 data logger; Onset Corporation, Massachusetts, USA), and Leveloggers (Levelogger 5 Junior;

168 Solinst Canada Ltd, Ontario, Canada), respectively. Perforated gauge tubes for the  
 169 levelloggers sealed with lids and soil temperature loggers were installed in 2020 inside the  
 170 collars at each plot.



171  
 172 Figure 3. Timeline of fertilization and harvest events applied to the 2-cut and 5-cut harvest  
 173 treatments during 2021-22.

174

175 **2.3 Net carbon dioxide and methane flux measurements**

176 The CO<sub>2</sub> and CH<sub>4</sub> measurements were performed biweekly +/- one week between 10:00 am  
 177 and 3:00 pm on days of predominantly clear sky conditions from 28 May 2021 to 14 June  
 178 2022. A total of 26 campaign measurements were undertaken. Fluxes were measured using a  
 179 fully transparent chamber (60 cm x 60 cm x 41 cm) made of Plexiglass and equipped inside  
 180 with a photosynthetic active radiation (PAR) sensor (190-SA; Li-Cor Inc., Lincoln, NE,  
 181 USA), a temperature sensor, and an air mixing fan. Further details of the chamber design and  
 182 how the temperature was controlled during operation can be found in Elsgaard et al. (2012).  
 183 The chamber was connected to an LGR-ICOS™ GLA131-GGA microportable gas analyzer  
 184 (ABB Ltd.), which simultaneously measured water vapor corrected CO<sub>2</sub> and CH<sub>4</sub> (i.e., dry  
 185 fractions) at 1 Hz resolution. Chamber deployment was 120 s per measurement. All data were  
 186 stored using a Campbell CR1000X data logger (Campbell Sci. Logan, UT, USA) with the  
 187 same timestamp. In order to fit the RCG inside the chamber during growth, a chamber

188 extension with the same dimensions as the measurement chamber was used during all  
189 measuring campaigns, i.e. total chamber height with the extension was 82 cm. Measurements  
190 were conducted during constant PAR conditions, when possible, by timing measurements  
191 such that changing cloud conditions were avoided. For each campaign and at each soil collar,  
192 fluxes were measured corresponding to four PAR levels by using net shrouds and an opaque  
193 cover as described by Kandel et al. (2017). This resulted in four flux measurements, one  
194 under fully transparent conditions which corresponded to net ecosystem exchange (NEE), a  
195 second under ca. 50% blocked PAR, a third under ca. 75% blocked PAR, and a fourth under  
196 100% blocked PAR equivalent to  $R_{eco}$ . Between PAR levels plants were given one minute to  
197 adapt to the new PAR conditions while the chamber was lifted on one side, allowing air  
198 circulation and bringing  $CO_2$  and  $CH_4$  concentrations to atmospheric levels.

199 All fluxes were calculated using the Flux package 0.3-0.1 (Jurasinski et al., 2022) in R (R  
200 Core Team (2023), R version 4.3.0). Inspection of fluxes revealed that fluxes were mostly  
201 linear, and flux rates were therefore calculated based on linear regression. For low  $CO_2$  fluxes  
202 ( $<100 \text{ mg } CO_2 \text{ m}^{-2} \text{ h}^{-1}$ ), fluxes with an  $R^2 < 0.6$  and a normalized root mean square error  
203 (NRMSE)  $> 0.1$  were removed, while for high  $CO_2$  fluxes ( $>100 \text{ mg } CO_2 \text{ m}^{-2} \text{ h}^{-1}$ ), fluxes with  
204 an  $R^2 < 0.9$  and a NRMSE  $> 0.1$  were identified and the PAR and  $CO_2$  flux were manually  
205 inspected. If sudden changes in the PAR occurred during the 2 min measurement period or if  
206 the flux curve indicated a possible leakage, flux data were discarded. These criteria resulted  
207 in 3% of the calculated  $CO_2$  fluxes being removed. In the case of  $CH_4$ , ebullitions were  
208 excluded by using the *fluxx* function of the Flux package, which automatically detects and  
209 excludes rapid concentration fluctuations while calculating fluxes. The resulting calculated  
210 linear  $CH_4$  fluxes had  $R^2$  values higher than 0.9, therefore no fluxes were removed based on  
211 non-linearity. If a possible leakage was identified by negative or non-linear  $R_{eco}$  fluxes, fluxes

212 were removed, resulting in 1.6% of the fluxes removed. For further calculations, only the  
213 CH<sub>4</sub> fluxes measured under 100% PAR blocked (opaque conditions) were used.

## 214 **2.4 Biomass measurements**

215 Spectral reflectance was measured in all collars biweekly at gas sampling days and before  
216 and after harvest events using a portable crop sensor (RapidSCAN CS-45; Holland Scientific  
217 Inc., Lincoln, NE, USA), which was held 30 cm above the canopy and horizontally rotated  
218 45° while performing measurements to cover all vegetation inside the collar. Approximately  
219 30 scans were taken per collar and their mean values were used to calculate the ratio  
220 vegetation index (RVI) as the ratio between the near-infrared and the red light reflectance.  
221 The RVI has been used as a proxy for photosynthetically active biomass and it has been used  
222 in photosynthesis and ecosystem respiration models (Kandel et al., 2017; Karki et al., 2019).  
223 Hourly RVI values were obtained by linearly interpolating biweekly RVI measurements, and  
224 used in GPP and R<sub>eco</sub> modelling. Fresh weight yield and dry matter content were determined  
225 by harvesting the biomass inside the collars at respective cuts and analyzed for total N and C  
226 with a Vario Max CN (Elementar Analysensysteme GmbH, Hanau, Germany). Dry matter  
227 yields (Table A1) were multiplied by percentage C to obtain the yield in C ha<sup>-1</sup> yr<sup>-1</sup> as part of  
228 the C budget. The sum of yields from individual cuts per treatment was considered as the  
229 annual yield.

## 230 **2.5 Gap filling models and annual budgets**

231 The measured NEE CO<sub>2</sub> fluxes were partitioned into GPP and R<sub>eco</sub>. The GPP was calculated  
232 for all PAR levels as NEE – R<sub>eco</sub>. From an atmospheric perspective we always consider R<sub>eco</sub>  
233 positive, and GPP negative while NEE can be either positive (ecosystem carbon source) or  
234 negative (ecosystem carbon sink). The net ecosystem carbon balance (NECB) was calculated  
235 as the sum of the NEE plus the harvested yields for the 2-cut and 5-cut treatments plus the

236 CH<sub>4</sub> emissions. For calculation of annual budgets, three models from previous studies (one  
 237 for GPP and two for R<sub>eco</sub>, see below) were used. Additionally, a fourth model was developed  
 238 based on a modification of the two selected R<sub>eco</sub> models. The GPP was modelled based on  
 239 Karki et al. (2019) (model 1).

$$240 \quad GPP = \frac{GPP_{max} * PAR}{k + PAR} * \left( \frac{RVI}{RVI + \alpha} \right) * FT \quad (\text{model 1})$$

241 where GPP is in mg CO<sub>2</sub> m<sup>-2</sup> h<sup>-1</sup>, *RVI* is the ratio vegetation index, *k* is the PAR value at  
 242 which GPP reaches 50%, *α* is a fitted parameter, and *FT* is a linear temperature dependent  
 243 function set to 0 when temperature < -2 °C and to 1 when temperature > 10 °C (Kandel et al.  
 244 2017).

245 R<sub>eco</sub> was modelled based on Karki et al. (2019) with *RVI* and *T<sub>s</sub>* as input variables (model 2),  
 246 based on Rigney et al. (2018) with *WTD* and *T<sub>s</sub>* as input variables (model 3), and with a new  
 247 model, which included *RVI*, *WTD* and *T<sub>s</sub>* as input variables (model 4).

$$248 \quad Reco = t1 + (a * RVI) * e^{\left[ b * \left( \frac{1}{T_{10} - T_0} - \frac{1}{T_s - T_0} \right) \right]} \quad (\text{model 2})$$

$$249 \quad Reco = t1 * e^{\left[ b * \left( \frac{1}{T_{10} - T_0} - \frac{1}{T_s - T_0} \right) \right]} + (WTD + c)^2 \quad (\text{model 3})$$

$$250 \quad Reco = t1 + (a * RVI) + [(WTD - WTD_{max}) * c]^2 * e^{\left[ b * \left( \frac{1}{T_{10} - T_0} - \frac{1}{T_s - T_0} \right) \right]} \quad (\text{model 4})$$

251 where R<sub>eco</sub> is in mg CO<sub>2</sub> m<sup>-2</sup> h<sup>-1</sup>, *RVI* is the ratio vegetation index, *WTD* is the water table  
 252 depth (cm), *WTD<sub>max</sub>* is the maximum *WTD* (cm), *t1*, *a*, *b*, and *c* are fitted parameters, *t1* has a  
 253 lower limit set at 1, while all other fitted parameters are without upper and lower limits. *T<sub>10</sub>* is  
 254 the reference temperature set to 10 °C, *T<sub>0</sub>* is the zero-respiration temperature set to -46 °C,  
 255 and *T<sub>s</sub>* is the soil temperature (°C) at 5 cm depth.

256

257 Each R<sub>eco</sub> model was fitted to data obtained biweekly using non-linear regression (non-least  
 258 square) in R (R Core Team (2023), R version 4.3.0) for each plot independently. Annual CO<sub>2</sub>  
 259 budgets were calculated using the parameterized models, hourly *T<sub>s</sub>*, *WTD*, and *RVI*. Model  
 260 performance was evaluated by comparing the measured GPP and R<sub>eco</sub> with the modelled  
 261 values using the following indices: Nash-Sutcliffe efficiency, which indicates how well the  
 262 plot of observed versus simulated data fits the 1:1 line, with more accurate models having

263 values closer to 1, corrected Akaike information criterion (AICc), normalized root mean  
264 square error, and  $R^2$  using the hydroGOF package in R (Zambrano-Bigiarini, 2020). Based on  
265 these criteria, the best performing  $R_{eco}$  model was used to calculate the annual  $CO_2$  budget. In  
266 addition, models of  $R_{eco}$  (model 4) and GPP were parameterized by pooling data from all  
267 blocks and treatment plots. The  $CH_4$  emissions were modelled using model 5 (Karki et al.  
268 (2014).

$$269 \quad CH_4 = (d1 + d2 * WTD) * e^{d3 * Ts} * (d4 + RVI) \quad (\text{model 5})$$

270 Where WTD is the water table depth,  $T_s$  is the soil temperature at 5 cm depth, RVI is the ratio  
271 vegetation index, and  $d_1$ ,  $d_2$ ,  $d_3$ , and  $d_4$  are fitted parameters.

272 We tested the sensitivity of the best performing  $R_{eco}$  model (model 4) to the frequency of  
273 WTD data either using (a) hourly WTD,  $T_s$ , and RVI (b) annual mean WTD with hourly  $T_s$   
274 and RVI, and (c) annual mean WTD, annual mean  $T_s$ , and hourly RVI.

## 275 **2.6 Water chemistry**

276 Soil pore water was collected biweekly at the same time as the gas campaigns and analyzed  
277 for total organic C (TOC), dissolved organic C (DOC), total nitrogen (TN), total dissolved  
278 nitrogen (TDN), nitrate-N, ( $NO_3$ ), ammonia-N ( $NH_4$ ), total P (TP), total dissolved P (TDP),  
279 Fe, pH, electrical conductivity (EC), and turbidity. Pore-water samples were collected  
280 immediately after each GHG measurement from the piezometers installed 20 cm from each  
281 GHG collar. Water samples were extracted with a syringe from a tube with the other end  
282 attached to an aquarium air stone (Air Stone Economy Cylinder 4 X 5 cm, Aquakoi / JV  
283 Trading Aps) placed 20 cm below the water table in each piezometer. An additional sample  
284 was collected from a ditch draining the peatland. A total of 13 samples were collected per  
285 campaign for a total of 338 samples. Upon collection, part of the sample was filtered using

286 0.45  $\mu\text{m}$  pore size filter. The unfiltered samples were analyzed for pH and electrical  
287 conductivity (EC) following the Danish Standards DS287 and DS288, respectively, turbidity,  
288 TN following Best (1976), TP using the Danish Standard, DS291 photometric method (Dansk  
289 Standard, 2004), TOC using a total organic C analyzer (TOC-VCPH; Shimatzu Corporation,  
290 Kyoto, Japan), and Fe by ICP emission spectrometer (iCAP 6000 series; Thermo Fisher  
291 Scientific, Inc., Walthman, Massachusetts, USA). The filtered samples were analysed for  
292 DOC with a (TOC-VCPH; Shimatzu Corpotation, Kyoto, Japan), TDN and  $\text{NO}_3$  (Best, 1976),  
293 TDP by the Danish Standard, DS291 photometric method (Dansk Standard, 2004), and  $\text{NH}_4$   
294 following Crooke and Simpson (1971).

## 295 **2.7 Statistical analysis**

296 Statistics were performed in R (R Core Team (2023), R version 4.3.0). Effects were  
297 considered significant if  $p \text{ value} < 0.05$ . Normality assumptions were evaluated with Q-Q  
298 plots, histograms, and residual plots. Kruskal-Wallis tests were used to test the effect of  
299 harvest treatment and block on  $R_{\text{eco}}$ , GPP, NEE, and NECB. Correlations and principal  
300 component analysis (PCA) were used to establish relationships between water chemistry  
301 parameters,  $R_{\text{eco}}$ , GPP, NEE, Ts, RVI, PAR, WTD, and  $\text{CH}_4$ .

302 ANOVA and Tukey tests were used to determine differences between water chemistry  
303 parameters among blocks and harvest treatments. The effects of each water chemistry  
304 parameter on  $R_{\text{eco}}$  and GPP were tested with linear mixed models. Each water chemistry  
305 parameter was added one by one as a fixed factor to the base models shown below as models  
306 5 and 6, and the performance of the model including each water chemistry parameter was  
307 compared to the base model. The  $R_{\text{eco}}$  base model included WTD, Ts, and RVI as fixed  
308 factors and the measuring campaign and replicate block as random factor (model 6), while

309 the GPP base model included PAR, Ts, and RVI as fixed factors and measuring campaign and  
310 replicate block as random factors (model 7).

311  $Reco = Harvest\ treatment + WTD + Ts + RVI + (campaign) + (R.Plot)$  (model 6)

312  $GPP = Harvest\ treatment + PAR + Ts + RVI + (campaign) + (R.Plot)$  (model 7)

313 Likelihood ratio tests were used to assess if the base models were significantly improved by  
314 adding a water chemistry parameter. If this was the case, the  $R^2$  and root mean square error  
315 (RMSE) were calculated. Outliers of the water chemistry data were identified as being larger  
316 than 3 times the standard deviation for each parameter independently excluding 1% of the  
317 data from the analyses.

### 318 **3. Results**

#### 319 **3.1 Carbon balance**

320 Management had a marginally significant effect on GPP (Kruskal-wallis test; p value < 0.1;  
321 n: 12), with more negative GPP (larger CO<sub>2</sub> uptake) in the 5-cut treatment ( $-20.2 \pm 0.7$  t CO<sub>2</sub>-  
322 C ha<sup>-1</sup> yr<sup>-1</sup>; mean  $\pm$  SE) and least negative in the 0-cut treatment ( $-15.5 \pm 1.3$  t CO<sub>2</sub>-C ha<sup>-1</sup> yr<sup>-1</sup>)  
323 (Table 2). No significant effects of management on R<sub>eco</sub> (between  $22.1 \pm 2.5$  and  $22.4 \pm 3.3$   
324 t CO<sub>2</sub>-C ha<sup>-1</sup> yr<sup>-1</sup>; p value = 0.98) and NEE (between  $2.2 \pm 0.5$  and  $6.9 \pm 2.2$  t CO<sub>2</sub>-C ha<sup>-1</sup> yr<sup>-1</sup>;  
325 p value = 0.22) were registered although the NEE of 0-cut was 4.6 t CO<sub>2</sub>-C ha<sup>-1</sup> yr<sup>-1</sup> higher  
326 than the two managed treatments on average. The 2-cut and 5-cut treatments gave similar  
327 annual biomass yields ( $4.0 \pm 0.7$  and  $3.8 \pm 0.2$  t C ha<sup>-1</sup> yr<sup>-1</sup>, respectively) leading to similar  
328 NECB for all treatments when the exported yields and CH<sub>4</sub> were added to the NEE (between  
329  $6.1 \pm 0.5$  and  $7.0 \pm 2.2$  t C ha<sup>-1</sup> yr<sup>-1</sup>). Biomass yields of the 2-cut treatment were similar for  
330 both harvesting events, but much lower in block A compared to the other blocks, while for the  
331 5-cut treatment yields peaked at the third harvest and were lowest at the fifth. There were less

332 yield differences between blocks for the 5-cut treatment compared to the 2-cut treatment.  
333 Block D had the highest yields of both 2-cut and 5-cut treatments.

334 Although the experimental site looked rather uniform, large differences were found between  
335 blocks, especially for Reco and NEE, the latter with coefficients of variation of 0.56, 0.71,  
336 and 0.41, for the 0-cut, 2-cut, and 5-cut, respectively. The lowest  $R_{eco}$  was registered in block  
337 A, followed by block B, and the highest  $R_{eco}$  was in blocks C and D ( $p < 0.05$ ) (Table 2, Fig 4).  
338 Differences in GPP between blocks were not significant despite lower  $CO_2$  uptake leading to  
339 lower biomass production in block A. No significant difference in NEE was observed  
340 between blocks because the higher  $R_{eco}$  was accompanied by larger  $CO_2$  uptake (more  
341 negative GPP) and thus higher biomass production. Figure 5 shows that the cumulative NEE  
342 grew faster in blocks C and D than in blocks A and B leading to approximately eight times  
343 higher annual NEE in blocks C and D compared to block A for the 0-cut treatment. The  
344 NECB was marginally different ( $p$  value  $< 0.1$ ) between blocks, with lowest NECB in block  
345 A, followed by block B, and highest in block C and D indicating that within field  
346 heterogeneity overrides treatments. However, the interaction between treatment and block  
347 indicated that harvest of biomass considerably reduced net  $CO_2$  emission in the more  
348 productive blocks (C and D) while little effect on NEE was seen for the less productive  
349 blocks (A and B) (Figure 5).

350 Cumulated methane emissions averaged  $90 \text{ kg CH}_4\text{-C ha}^{-1} \text{ yr}^{-1}$  for the studied year and varied  
351 primarily by block with less emissions at block C and largest emissions at block A (Table 2  
352 and Fig. A4). Methane had no significant correlations with nutrients (Fig. A1), except  $NH_4$ ,  
353 which had a negative correlation with  $CH_4$ .  $CH_4$  also had a positive correlation with  $R_{eco}$  and  
354 Ts but no significant correlation with WTD.

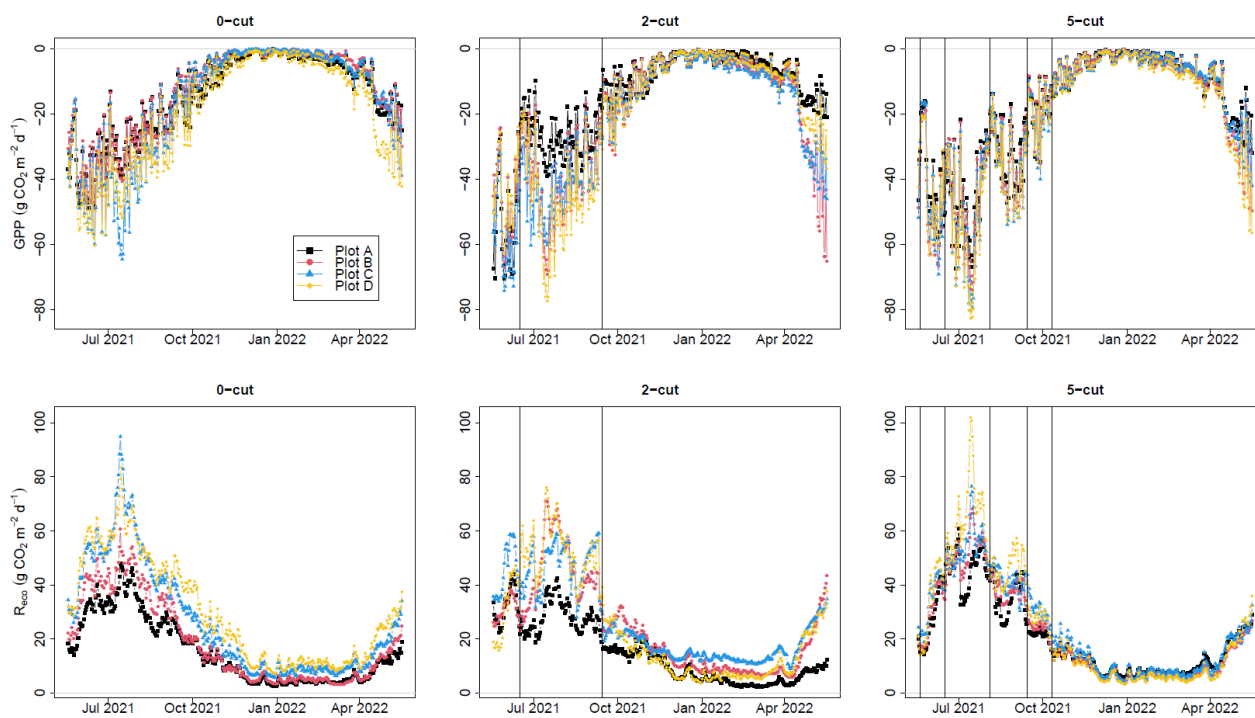
355 Table 2. Cumulated C emission for the four studied blocks and harvest treatments during the  
 356 study year.

Block	Treatment	Reco	GPP	NEE	Yield	CH <sub>4</sub>	NECB	GWP
		t CO <sub>2</sub> -C ha <sup>-1</sup>	t CO <sub>2</sub> -C ha <sup>-1</sup>	t CO <sub>2</sub> -C ha <sup>-1</sup>	t C ha <sup>-1</sup>	t CH <sub>4</sub> -C ha <sup>-1</sup>	t C ha <sup>-1</sup>	t CO <sub>2</sub> e ha <sup>-1</sup>
A	0	15.4	-14.2	1.2	NA	0.15	1.3	8.9
B		18.6	-13	5.6	NA	0.10	5.7	23.5
C		26.2	-16	10.2	NA	0.03	10.2	38.3
D		29.4	-18.9	10.6	NA	0.09	10.7	41.5
mean ± SE		22.4 ± 3.3	-15.5 ± 1.3	6.9 ± 2.2	NA	0.09 ± 0.02	7 ± 2.2	28.1 ± 7.5
A	2	14.9	-15.3	-0.4	1.9	0.12	1.6	9.1
B		23.6	-20.8	2.8	4.5	0.09	7.4	29.5
C		26.4	-22	4.3	4.6	0.04	9.0	34.1
D		23.7	-20.6	3.1	5	0.14	8.2	34.1
mean ± SE		22.1 ± 2.5	-19.7 ± 1.5	2.5 ± 1	4.0 ± 0.7	0.1 ± 0.02	6.6 ± 1.7	26.7 ± 6.0
A	5	20.6	-18.5	2.2	3.5	0.10	5.7	23.7
B		21	-20.2	0.8	3.9	0.08	4.8	19.5
C		23.7	-20.4	3.3	3.5	0.06	6.9	26.7
D		24.3	-21.9	2.4	4.5	0.06	7.0	27.1
mean ± SE		22.4 ± 0.9	-20.2 ± 0.7	2.2 ± 0.5	3.8 ± 0.2	0.08 ± 0.01	6.1 ± 0.5	24.3 ± 1.8

357

358 R<sub>eco</sub> is ecosystem respiration, GPP is gross primary productivity, NEE is net ecosystem  
 359 exchange, NECB is net ecosystem carbon balance (NEE + yield + CH<sub>4</sub>), and GWP is the  
 360 global warming potential (NECB + CH<sub>4</sub>) in CO<sub>2</sub> equivalent units.

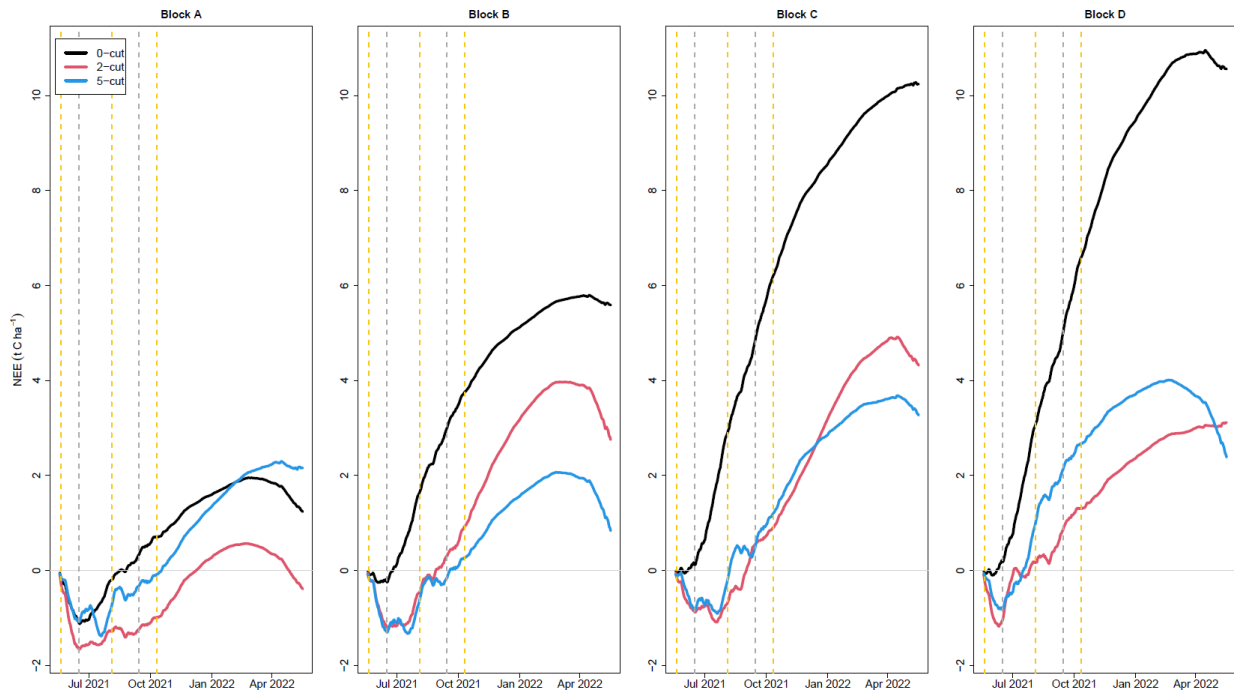
361



362

363 Figure 4. Modelled daily gross primary productivity (GPP) (top) and ecosystem respiration  
364 ( $R_{\text{eco}}$ ) (bottom) for the three management treatments (0-cut, 2-cut, and 5-cut). Colors indicate  
365 the four block replicates. Vertical lines are harvesting events.

366



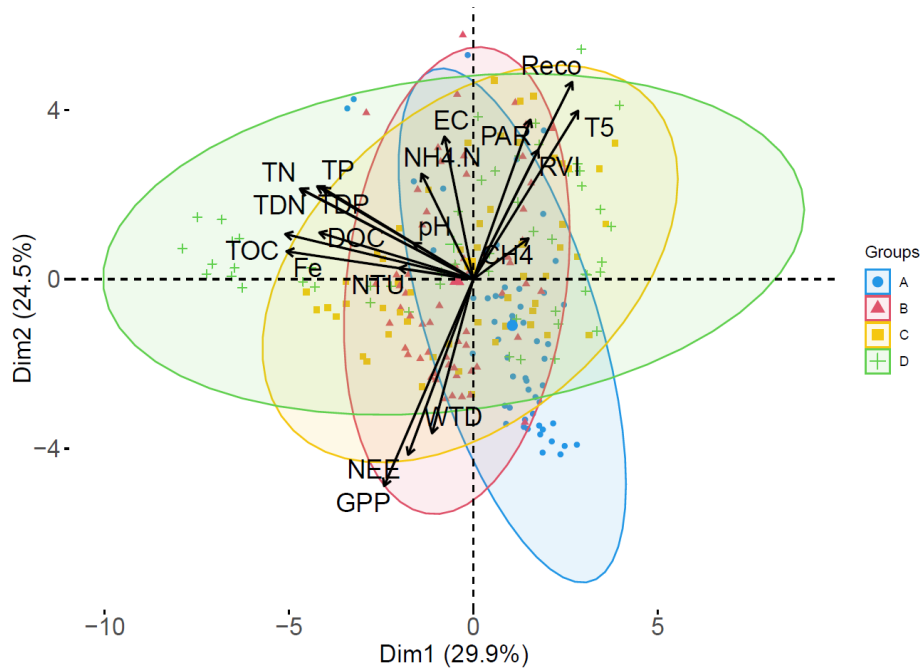
367

368 Figure 5. Cumulative net ecosystem exchange for the four studied blocks and three harvest  
 369 treatments. Black line is the 0-cut, red line is the 2-cut, and blue line is the 5-cut.  
 370 Vertical gray dashed lines are harvest events for only the 2-cut treatment while all vertical  
 371 dashed lines are harvest events for both the 2-cut and 5-cut treatments.

### 372 3.2 Model performance

373 Measured  $R_{eco}$  was best described by model 4 in 11 out of the 12 studied plots based on the  
 374 Nash-Sutcliffe model efficiency (NSE) and in 10 out of 12, based on the AICc (table A3). The  
 375 other calculated indices ( $R^2$ , and NRMSE) also supported model 4 as the best overall  
 376 performing model. Additional 1:1 plots of measured vs. modelled  $R_{eco}$  for model 4 can be  
 377 seen in Figure A3 in appendix. When WTD was excluded as seen in model 2 compared to  
 378 model 4, the overall performance was reduced as indicated by lower NSE for most plots  
 379 except for plot C 5-cut and plot D 0-cut (Table A3). Model 3, where RVI was excluded, had  
 380 the lowest performance of the three tested models. In general, the 0-cut plots provided the  
 381 best model performances (highest NSE),  $R^2 > 0.9$ , and the lowest AICc, while the 2-cut and  
 382 5-cut plots had lower model performances (between 0.74 and 0.92 NSE). The performance  
 383 results for the GPP models had  $R^2$  values that ranged between 0.81 and 0.96 (Table A3).

384  $R_{\text{eco}}$  was positively correlated with  $T_s$  and RVI, and negatively correlated with WTD (lower  
385 WTD = deeper water table). On the other hand, GPP was negatively correlated to  $T_s$ , RVI,  
386 and PAR, meaning that larger  $T_s$ , RVI, and PAR correlate to larger  $\text{CO}_2$  uptake. These  
387 expected relationships seen in the PCA plot (Fig 6) and correlations statistics (Fig. A1)  
388 support why the variables in models 1-4 were selected and parameterized in this study. The  
389 fitted parameter values of the best performing  $R_{\text{eco}}$  model and the GPP model varied between  
390 plots (Fig A2). For the  $R_{\text{eco}}$  model, the  $b$  parameter was near its maximum value in most  
391 plots, while for the GPP model, the  $k$  parameter was near its maximum in most plots.



392

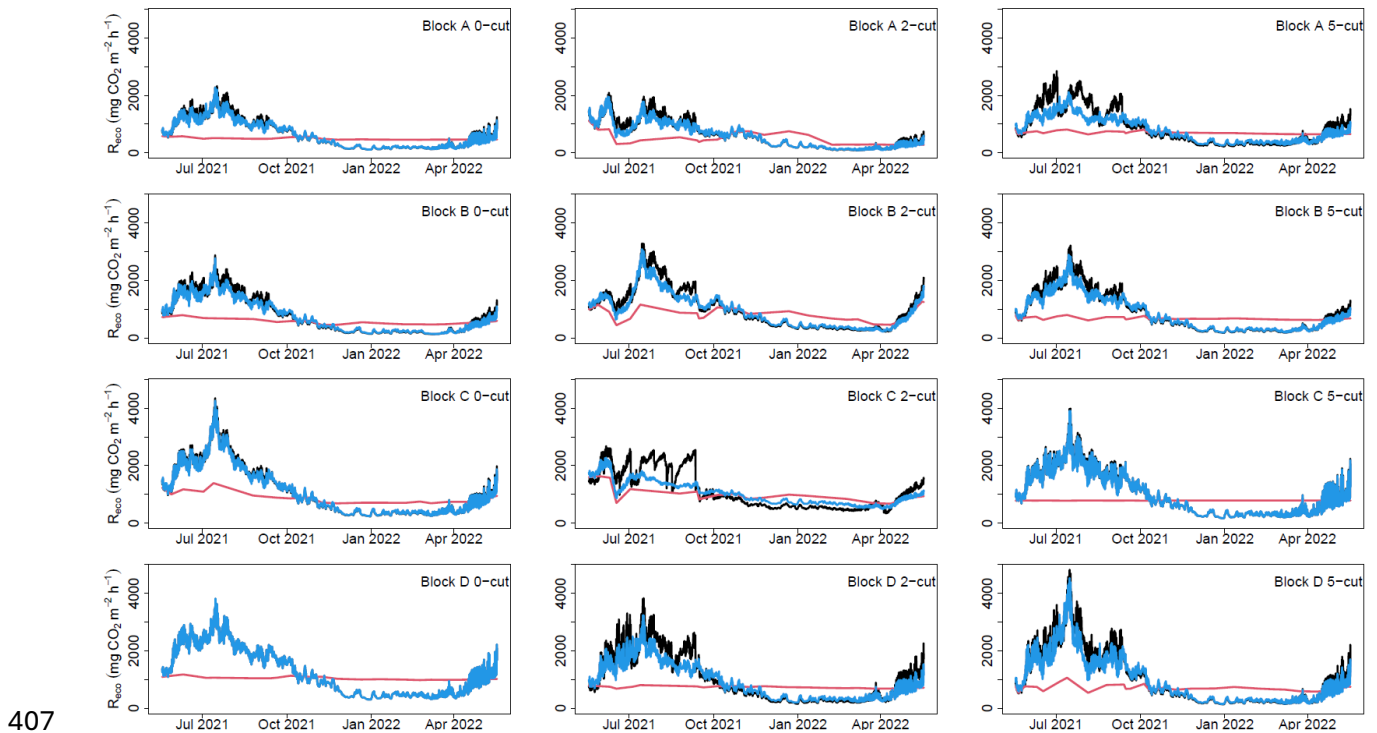
393 Figure 6. Principal component analysis PC1 vs PC2 plot. Variability explained by each PCA  
 394 is the value in parenthesis. Colors represent the four studied blocks. Harvest treatments are  
 395 combined.

396

### 397 3.3 Sensitivity analysis using WTD with different temporal resolution

398 Using annual mean WTD and  $T_s$  as input for model 4 instead of hourly values,  
 399 underestimated  $R_{eco}$  between 9 to 26% for all plots with an average of 18% (Fig 7) (Table  
 400 A4). On the other hand, using the annual mean WTD along with hourly  $T_s$  generally followed  
 401 similar trends in  $R_{eco}$  as using hourly input data, but high emission events were slightly  
 402 underestimated resulting in an underestimation that ranged between 0 and 10% with an  
 403 average of 5% for all plots when compared to the model that used hourly data (Fig 7) (Table  
 404 A4). If the  $R_{eco}$  was calculated using annual mean WTD and annual mean  $T_s$ , or annual mean  
 405 WTD along with hourly  $T_s$ , the C budget resulted in a total mean NECB of 2.7 and 5.4 t C ha<sup>-1</sup>

406  $\text{yr}^{-1}$ , respectively.



407

408 Figure 7. Sensitivity of ecosystem respiration ( $R_{\text{eco}}$ ) modelled for all plots to the data  
409 frequency of water table depth (WTD). Black lines represent  $R_{\text{eco}}$  modelled with hourly  
410 WTD, soil temperature ( $T_s$ ), and RVI, blue line represents  $R_{\text{eco}}$  modelled with mean annual  
411 WTD, hourly  $T_s$ , and hourly RVI, and red line represents  $R_{\text{eco}}$  modelled with mean annual  
412 WTD, mean annual  $T_s$ , and hourly RVI.

### 413 3.4 Water chemistry

414 The PCA described in total 67.8 % of the variance in data by the first three principal  
415 components. PC1 and PC2 explained 29.9 and 24.7% of the variability in the data,  
416 respectively, while PC3 explained 13.4% of the variability. The PC1 VS PC2 plot (Fig 6)  
417 shows clustering of the data with block D and A having the largest difference. PC1 describes  
418 the pore water nutrients, which are positively correlated with each other, and significance of  
419 correlations are presented in Figure A1. This shows that WTD had positive correlations with  
420 Fe, TOC and DOC and negative correlations with  $\text{NH}_4$  and TDP, while  $T_s$  had negative  
421 correlations with all nutrients except  $\text{NH}_4$  and TDP. Predominant correlations of nutrients  
422 with  $R_{\text{eco}}$  were negative and positive with GPP and NEE, respectively.

423 Comparisons of water chemistry parameters between blocks indicated significant differences  
 424 depending on type of nutrients. Generally, block (A) had the lowest nutrient concentrations,  
 425 while block (D) had the highest nutrient concentrations, with the exception of DOC. The  
 426 nutrient concentrations at the ditch appeared lower than the concentrations in the soil pore  
 427 water at the blocks except for the TP and TDP (Table 3). Comparisons between harvest  
 428 treatments showed that the 2 and 5-cut treatments had higher N and Fe concentrations than  
 429 the 0-cut treatment, while there were no differences in other nutrients (Table 3). Additionally,  
 430 the interaction between harvest treatment and block was significant for NH<sub>4</sub>, electrical  
 431 conductivity, pH, and turbidity.

432 The linear mixed model (Model 6) indicated that all nutrient concentrations, except NH<sub>4</sub>,  
 433 significantly improved the base R<sub>eco</sub> model, however the effect of TP, TDP, and pH also  
 434 varied at plot level. For GPP, the addition of nutrient concentrations into the model did not  
 435 improve the base models, however pH and EC improved model 7 with its effect varying at  
 436 plot level. The magnitude of model improvement (higher R<sup>2</sup> and lower RMSE) was larger for  
 437 R<sub>eco</sub> than for GPP, however, in general the R<sup>2</sup> and RMSE did not change considerably for all  
 438 nutrients/parameters compared to the base models (Table A5).

439 Table 3. Mean annual concentrations of water chemistry parameters at block A, B, C, and D,  
 440 and treatments 0-cut, 2-cut, and 5-cut.

Block	pH	EC	Turbidity	TOC	DOC	TN	TDN	NH <sub>4</sub> -N	NO <sub>3</sub> -N	TP	TDP	Fe
		mS cm <sup>-1</sup>	NTU	mg L <sup>-1</sup>	mg L <sup>-1</sup>	mg L <sup>-1</sup>	mg L <sup>-1</sup>	mg L <sup>-1</sup>	mg L <sup>-1</sup>	mg L <sup>-1</sup>	mg L <sup>-1</sup>	mg L <sup>-1</sup>
A	5.61 ± 0.05 (a)	0.19 ± 0.01 (a)	25.4 ± 2.01 (ab)	164 ± 9 (a)	129 ± 7 (a)	14.1 ± 0.9 (a)	12.8 ± 0.8 (a)	1.56 ± 0.25 (a)	4.98 ± 3.18	0.49 ± 0.04 (a)	0.40 ± 0.04 (a)	12.2 ± 0.9 (a)
B	6.40 ± 0.04 (c)	0.34 ± 0.01 (c)	29.6 ± 2.95 (b)	212 ± 7 (b)	160 ± 5 (b)	16.8 ± 0.4 (b)	15.5 ± 0.5 (b)	1.50 ± 0.15 (a)	1.38 ± 0.58	0.81 ± 0.04 (c)	0.69 ± 0.05 (b)	22.9 ± 1.1 (b)
C	6.22 ± 0.04 (b)	0.34 ± 0.01 (b)	40.3 ± 3.76 (c)	193 ± 10 (b)	135 ± 6 (ab)	18.6 ± 0.9 (b)	16.2 ± 0.7 (b)	3.34 ± 0.29 (b)	2.97 ± 1.49	0.68 ± 0.04 (b)	0.50 ± 0.03 (a)	19.0 ± 1.6 (b)
D	6.25 ± 0.04 (b)	0.32 ± 0.01 (b)	26.7 ± 3.85 (a)	209 ± 16 (b)	137 ± 8 (a)	19.6 ± 1.2 (b)	18.9 ± 1.2 (b)	2.95 ± 0.24 (b)	3.58 ± 1.90	1.07 ± 0.08 (c)	0.91 ± 0.08 (b)	36.3 ± 3.6 (c)
ditch	6.65 ± 0.07	0.32 ± 0.01	41.9 ± 32.9	66 ± 8	42 ± 3	7.2 ± 1.8	4.6 ± 0.3	1.2 ± 0.2	1.09 ± 0.21	1.13 ± 0.23	0.93 ± 0.2	3.9 ± 1.1
<b>Treatment</b>												
0	6.13 ± 0.05 (b)	0.26 ± 0.01 (a)	27.3 ± 2.4	191 ± 9	137 ± 5	16.0 ± 0.8 (a)	14.5 ± 0.7 (a)	1.96 ± 0.16 (a)	0.15 ± 0.03	0.83 ± 0.06	0.63 ± 0.05	20.3 ± 1.9 (a)
2	6.04 ± 0.05 (a)	0.31 ± 0.01 (b)	33.3 ± 3.0	189 ± 10	136 ± 6	18.5 ± 0.9 (b)	16.9 ± 0.9 (b)	2.69 ± 0.30 (b)	7.49 ± 2.64	0.71 ± 0.04	0.59 ± 0.05	23.3 ± 1.9 (b)

441

442 Total organic carbon (TOC), dissolved organic carbon (DOC), total nitrogen (TN), total  
 443 dissolved nitrogen (TDN), ammonia (NH<sub>4</sub>-N), nitrate (NO<sub>3</sub>-N), total phosphorus (TP), total  
 444 dissolved phosphorus (TDP), electrical conductivity (EC). Values are means ± standard error.  
 445 N values are 78, 25, and 104 for the blocks, ditch, and treatments, respectively. Letters in  
 446 parenthesis indicate significant differences between block (top) and harvest treatments  
 447 (bottom). The ditch was not included in statistical comparisons. No comparisons were  
 448 performed for NO<sub>3</sub> due to insufficient data.

449

450

## 451 **4. Discussion**

### 452 **4.1 Carbon balance**

#### 453 **4.1.1 Annual budgets**

454 Comparison of results from this study to previous flux measurements on managed Danish  
 455 peatlands presented by Koch et al. (2023) shows that the total mean CO<sub>2</sub>-C emissions (NEE  
 456 + yield) from this study (6.5 t CO<sub>2</sub>-C ha<sup>-1</sup> yr<sup>-1</sup>) are larger than emissions from other Danish  
 457 organic soils under fertilization and similar WTD (between 0 and 2.5 t CO<sub>2</sub>-C ha<sup>-1</sup> yr<sup>-1</sup>; Koch  
 458 et al., 2023). Similarly, our total mean NECB (6.6 t C ha<sup>-1</sup> yr<sup>-1</sup>) is larger than emissions from  
 459 peatlands at similar WTD from both Germany (between -1.0 t C ha<sup>-1</sup> yr<sup>-1</sup> and 1.5 t C ha<sup>-1</sup> yr<sup>-1</sup>;  
 460 Tiemeyer et al., 2020) and the UK (between -2.0 t C ha<sup>-1</sup> yr<sup>-1</sup> and 0.8 t C ha<sup>-1</sup> yr<sup>-1</sup>; Evans et al.,  
 461 2021). Nielsen et al. (2024) reported the effect of management on GHG emissions from 2020  
 462 to 2021 at the same study site as reported here, and found a higher mean NECB of 9.4 t C ha<sup>-1</sup>  
 463 yr<sup>-1</sup> at the slightly lower mean annual WTD of -10 cm. Although mean annual WTD  
 464 increased only 2 cm, not maintaining the drainage ditches resulted in considerably higher  
 465 WTD during summer 2021 envisaged by temporary flooded conditions. Higher WTD along  
 466 with a reduction of WTD fluctuations as rewetting progresses (Karimi et al., 2024), could  
 467 explain the lower NECB in 2021-22 compared to 2020-21 (Fig 2A). Other studies have also  
 468 shown a delay in reaching carbon neutral conditions despite drainage being stopped (Hemes

469 et al., 2019; Kreyling et al., 2021). For the shallow annual mean WTD registered at our study  
470 site we expected lower CO<sub>2</sub> emission according to IPCC Tier 1 emission factors. However,  
471 here R<sub>eco</sub> is likely driven by the dynamic interaction of a drop in WTD during summer  
472 coinciding with maximum Ts. This naturally stimulated CO<sub>2</sub> production in the peat and  
473 together with plant respiration drove the high annual R<sub>eco</sub> (Fig 4).

474 Mean CH<sub>4</sub> emissions from this study were within the range of emissions from pristine and  
475 rewetted Danish and German peatlands reported by Koch et al. (2023) and Tiemeyer et al.  
476 (2020) (between 75 and 150 kg CH<sub>4</sub>-C ha<sup>-1</sup> yr<sup>-1</sup>, approximately) and no treatment effect was  
477 apparent. We found that CH<sub>4</sub> emissions contributed 11.7% to total net mean NECB  
478 expressed as CO<sub>2</sub>e, using global warming potential (GWP) = 27 for CH<sub>4</sub> (Foster et al., 2021).  
479 Peatland rewetting is expected to reduce CO<sub>2</sub> emissions while simultaneously increasing CH<sub>4</sub>  
480 emissions (Abdalla et al., 2016; Darusman et al., 2023). Thus, further monitoring of CH<sub>4</sub>  
481 emissions would be needed as rewetting progresses at the study site.

#### 482 **4.1.2 Management effect on CO<sub>2</sub> emissions**

483 Rewetted nutrient-rich fen peatlands have higher CO<sub>2</sub> emissions compared to low-nutrient  
484 ones (Wilson et al., 2016). Management alternatives to reduce emissions from these sites are  
485 therefore needed in order to meet emission reduction targets. Paludiculture has been found to  
486 effectively reduce emissions from rewetted peatlands (Tanneberger et al., 2020; De Jong et  
487 al., 2021; Bockermann et al., 2024), but type of paludiculture crop seems important for the  
488 reduction potential (Lång et al., 2024). Our results showed that after three years of  
489 establishment and management of RCG at the study site, NECB was not significantly  
490 different compared to no management. These results support findings by Nielsen et al. (2024)  
491 who found no effect of management on GHG emissions during the second year (2020) after  
492 RCG establishment at the study site. The NECB assumes that all harvested biomass is

493 converted to CO<sub>2</sub> when removed from the field. However, if the biomass is considered as a  
494 resource potentially reducing the use of fossil fuels, comparison of NEE among treatments  
495 would also be a relevant measure. Based on NEE, we found a potential emission reduction of  
496 4.5 and 4.7 t CO<sub>2</sub>-C ha<sup>-1</sup> yr<sup>-1</sup> for the 2 and 5-cut management strategies, respectively, in  
497 comparison to no management, but this difference was not significant because of large  
498 variation between treatment replicates especially for the 0-cut. Our NEE estimates were  
499 lower for all treatments compared to Nielsen et al. (2024). We attribute this reduction in net  
500 CO<sub>2</sub> emissions not only to the reduction in biomass production but also to the rewetting  
501 process, which lowered heterotrophic peat mineralization.

502 A life cycle assessment of RCG on fen peatlands by Thers et al. (2023) showed that fuel  
503 consumption during harvesting can make up a considerable amount of GHG emissions  
504 associated to management. Since no considerable difference in yields were found between the  
505 2-cut and 5-cut treatments, and a progressive decline was seen after the third harvest of the 5-  
506 cut treatment, we would recommend the 2-cut management for RCG in peatlands such as the  
507 study site to maximize harvest efficiency and to minimize disturbance to the peatland.

508 Although yields of 2021 (8.9 and 8.6 t DM ha<sup>-1</sup>) (Table A1) were acceptable they were  
509 considerably lower compared to 2019 yields (15.6 and 14.9 t DM ha<sup>-1</sup>) (Nielsen et al., 2021)  
510 and to 2020 yields (12.7 and 13.8 t DM ha<sup>-1</sup>) (Nielsen et al., 2023a) for the 2-cut and the 5-  
511 cut, respectively. The amount of N removed in the harvested biomass was on average 206 kg  
512 N ha<sup>-1</sup> and slightly lower in the 2-cut compared to the 5-cut (Table A2), therefore, the same  
513 amount of N applied as fertilizer was removed at harvest. However, we found generally  
514 higher concentrations of N forms in pore water at the 2 and 5-cut treatments compared to the  
515 0-cut treatment. A complete assessment of the N balance would help to determine the full  
516 environmental benefit of RCG as paludiculture.

#### 517 **4.1.3 Paludiculture and potential CO<sub>2</sub> mitigation**

518 In the most productive blocks of the experiment, paludiculture seemed to accelerate the  
519 reducing effect of rewetting on CO<sub>2</sub> emission. Higher R<sub>eco</sub> and marginally higher NECB were  
520 measured in blocks C and D, which in this study were also the areas with higher porewater  
521 nutrient concentrations compared to R<sub>eco</sub> and NECB measured in the block A. The difference  
522 in emissions between no harvest (0-cut) and harvest (2 or 5-cut) for the highly productive  
523 blocks (C and D) were on average 7.1 t CO<sub>2</sub>-C ha<sup>-1</sup> yr<sup>-1</sup> based on NEE and 2.7 t C ha<sup>-1</sup> yr<sup>-1</sup>  
524 based on NECB. However, in areas of less emissions (block A in this study), paludiculture  
525 would be less recommended because differences were not apparent for harvested and non-  
526 harvested plots and relatively small yields could be harvested as a biomass resource. These  
527 results stress the importance of acknowledging peatland heterogeneity in rewetting with  
528 paludiculture projects to maximize emission reductions.

#### 529 **4.2 Peatland heterogeneity**

530 Even though the studied area was relatively small (3.9 ha) and appeared to be uniform, we  
531 found differences in CO<sub>2</sub> emissions and porewater nutrients among the studied blocks. Peat  
532 chemistry data (Table 1) also indicated differences in pH, organic matter content, and TC  
533 among the studied blocks which might be related to the peat forming process. The peatland  
534 heterogeneity might have originated from differences in topography, groundwater flow, and  
535 vegetation variability, leading to variable rates of peat and C accumulation (Piilo et al., 2020),  
536 and R<sub>eco</sub> (Juszczak et al., 2013). which affected the pore water nutrient concentrations,  
537 microbial communities and GHG balance (Arsenault et al., 2019; Chronakova et al., 2019;  
538 Kou et al., 2020). Mashadi et al. (2024) found, at the same location where this study was  
539 conducted, an increasing degree of peat decomposition approaching the stream, therefore,  
540 higher nutrient concentrations in blocks closer to the stream could be explained by higher  
541 peat decomposition and organic matter mineralization at this area. Heterogeneity at the study  
542 site was also reflected by considerable variability in values of the fitted parameters of the R<sub>eco</sub>

543 and GPP models (Fig A2). Pooling all data to obtain field  $R_{\text{eco}}$  and GPP models resulted in  
544 lower model efficiencies (Table A6) compared to the approach of modelling each plot  
545 separately and led to similar  $R_{\text{eco}}$ , GPP, and NEE among treatments and blocks (Table A7).

#### 546 **4.3 Sensitivity of $R_{\text{eco}}$ prediction to temporal resolution of WTD**

547 In previous studies, mean annual WTD have been used as the only predictor for NECB, but  
548 not without considerable variation in data points used to build these relationships (Tiemeyer  
549 et al., 2020; Evans et al., 2021; Koch et al., 2023). We found that information on Ts, RVI and  
550 PAR improved prediction as they have large impact on GPP and  $R_{\text{eco}}$ . The other two models  
551 evaluated (models 2 and 3) also included Ts as explanatory variable. Temperature is a major  
552 soil respiration driver (Silvola et al., 1996; Lafleur et al., 2005; Rigney et al., 2018) as higher  
553 soil temperatures increase microbial activity and soil respiration but it depends also on water  
554 table and soil moisture (Silvola et al., 1996; Lafleur et al., 2005). Out of the three  $R_{\text{eco}}$  models  
555 we tested, the combined model including RVI, WTD and Ts performed best (model 4). When  
556  $R_{\text{eco}}$  was estimated by models 2 or 3, where either RVI or WTD was omitted the annual  $R_{\text{eco}}$   
557 and thus NECB was underestimated by 8.9 and 3.5%, respectively. Therefore, model  
558 selection is important to accurately estimate  $\text{CO}_2$  emissions from peatlands.

559 In this study, Ts captured major trends in  $R_{\text{eco}}$ . This can be seen by the importance of the  
560 fitted Ts parameter ( $b$ , model 4) (Fig A2) and by results shown in Figure 7, in which hourly  
561 Ts along with mean annual WTD captured most  $R_{\text{eco}}$  trends, However, this model  
562 underestimated  $R_{\text{eco}}$  by an average of 5%, which would be equivalent to an NECB  
563 underestimation of  $1.2 \text{ t C ha}^{-1} \text{ yr}^{-1}$  compared to the model with hourly WTD and hourly Ts.  
564 The use of mean annual WTD and mean annual Ts resulted in an even larger NECB  
565 underestimation ( $3.9 \text{ t C ha}^{-1} \text{ yr}^{-1}$ ) compared to the hourly model. This underestimation is due  
566 to the combined effect of lower WTD and higher Ts during summer on  $R_{\text{eco}}$ , which is not

567 captured when mean WTD and Ts are used. The model based on hourly WTD and Ts also  
568 improved simulation of  $R_{eco}$  peaks (Figs 8 and A2), which might be of great importance under  
569 extreme weather and climate change conditions. Juszczak et al (2013) also found that the  
570 response of  $R_{eco}$  to Ts can be influenced by WTD and that models including both WTD and  
571 Ts provide a better representation of  $R_{eco}$  in heterogeneous peatlands. Emission factors  
572 derived from models based on annual mean WTD, such as those currently used for rewetted  
573 peatlands would underestimate  $R_{eco}$  when applied to peatlands with fluctuating and lower  
574 WTD during the warm season. This is an important observation particularly for rewetted  
575 peatlands, which might take years to achieve hydrological stability (Kreyling et al., 2021).  
576 Improved  $CO_2$  modelling therefore requires information on fluctuating WTD possibly  
577 obtained from hydrological modelling if measurement data are unavailable.

#### 578 **4.4 Effect of nutrients in $CO_2$ emissions**

579 Positive correlations between porewater nutrients suggest common drivers for their release.  
580 Concentrations of dissolved organic matter components have been found to correlate with  
581 concentrations of metals in Canadian bogs (Bourbonniere, 2009). Peat mineralization has  
582 been found to be a major driver of nutrient release from drained peatlands (Cabezas et al.,  
583 2013; Haapalehto et al., 2014). Predominantly higher nutrient concentrations at the studied  
584 blocks compared to the ditch indicate differences between the pore water (measured at the  
585 plots) and the groundwater (measured at the ditch), suggesting that peat mineralization and  
586 fertilization are larger pore water nutrient sources compared to groundwater. Peat nutrient  
587 concentrations and pH have been found to be potential indicators for GHG emissions in  
588 rewetting peatlands (Nielsen et al., 2023b). We showed that the prediction of  $R_{eco}$  was  
589 improved when soil pore water chemistry data were included in addition to WTD, RVI and Ts  
590 as fixed factors. Although, the magnitude of this improvement was small based on the  $R^2$   
591 increase (between 0.004 and 0.015 depending on the pore water chemistry parameter), this

592 indicated a relation between mineralization and porewater nutrients at the study site. The  
593 exact influence of nutrients on  $R_{eco}$  should be further investigated. In this study we measured  
594 nutrient concentrations but not nutrient load, which is the total mass of a nutrient and can be  
595 more informative about the nutrient status of the peatland (Cabezas et al., 2013). Under  
596 higher (shallower) WTD, nutrient concentrations can be diluted (Griffiths et al., 2019).  
597 Positive correlations between WTD and TOC, DOC and Fe could be due to release of DOC  
598 accumulated under drained summer conditions and increase in Fe solubility under higher  
599 water tables (Haapalehto et al., 2014).

600 Previous studies have explored variability on water chemistry between and within peatlands  
601 (Bourbonniere, 2009; Wood et al., 2016; Arsenault et al., 2018; Griffiths et al., 2019).

602 Nutrient concentrations in peatland's porewater are affected by several factors including  
603 water table depth, temperature, peat decomposition degree, and redox (Bourbonniere, 2009;  
604 Cabezas et al., 2013; Haapalehto et al., 2014; Wood et al., 2016); Furthermore, nutrient  
605 concentrations, base cations, and pH change upon peatland rewetting (Lundin et al., 2017).

606 For this study, WTD was generally lower in blocks C and D (Fig 2B). Malinowski et al.  
607 (2015) found that the area where block A is located is more responsive to changes in the  
608 stream water level due to its proximity to the drainage ditch, which might have caused the  
609 higher mean WTD in this block. Additionally, differences in mobile porosity at the study site  
610 might have made some areas more prone to be affected by changes in WTD than others  
611 (Mashadi et al., 2024). Minor differences in WTD between the replicate blocks could have  
612 produced a different degree of exposure to incoming water sources. Nutrient concentrations  
613 in incoming water sources can in turn affect pore water nutrient concentrations (Bridgham  
614 and Richardson, 1993; Cabezas et al., 2013), which could have contributed to differences  
615 found between blocks, additionally, higher WTD in block A could explain lower nutrient  
616 concentrations due to dilution. The minor differences found in WTD might increase peat

617 mineralization in drier blocks resulting in higher DOC and N concentrations (Arsenault et al.,  
618 2018; Haapalehto et al., 2014; Wood et al., 2016). Nutrient additions have been found to  
619 increase  $R_{eco}$  in peat soils (Larmola et al., 2013). Higher mineralization and larger nutrient  
620 release from organic matter decomposition at lower WTD blocks could explain differences in  
621  $CO_2$  emissions among replicate blocks as evidenced by higher mineralization and  $R_{eco}$  found  
622 at blocks C and D. Higher plant productivity and fresh decomposable organic matter  
623 contributes to higher nutrient concentrations found in rewetted peatlands (Haapalehto et al.,  
624 2014), which could explain higher N concentrations found in blocks C and D. This is also  
625 supported by marginally higher NECB found in these blocks compared to blocks A and B ( $p$   
626  $< 0.1$ ). Nutrients released from the decomposing vegetation have been found to increase soil  
627 respiration and mineralization in high-nutrient peat soils (Larmola et al., 2013). A feedback  
628 mechanism by which higher mineralization and nutrient release enhances plant productivity,  
629 which in turn increases fresh organic matter inputs into the soil and further nutrient releases  
630 could drive high nutrient concentrations in poorly drained fen peatlands such as this one.

#### 631 **4.5 Considerations for the potential use of RCG harvested biomass**

632 In order to reestablish the C sink function of rewetted peatlands, peat formation would need  
633 to be reestablished, however, reaching this state may take decades (Kreyling et al., 2021).  
634 Paludiculture provides an opportunity to achieve indirect GHG emission reductions by  
635 replacing fossil fuels, however, since harvested biomass C makes out a considerable amount  
636 of GHG emissions from cultivated RCG in fen peatlands because it is considered as a  $CO_2$   
637 emission immediately after harvest according to IPCC guidelines (Thers et al., 2023), the end  
638 use of the harvested biomass is key to achieve the potential GHG mitigation. Reed canary  
639 grass grown in wet Danish fen peatlands was shown suitable for protein extraction as  
640 supplement in the diets of monogastric animals and side strips or all the harvested biomass  
641 could be used for biogas production thereby replacing fossil fuels (Kandel et al., 2013;

642 Nielsen et al. 2021; Nielsen et al., 2023a). Since N<sub>2</sub>O was not measured in the present study,  
643 further information is needed to assess the extent of N<sub>2</sub>O contribution to GHG emissions  
644 given that N fertilization for RCG can increase N<sub>2</sub>O emissions in fen peatlands (Kandel et al.,  
645 2019). However, N<sub>2</sub>O emissions equivalent to 1.4 t CO<sub>2</sub>e ha<sup>-1</sup> yr<sup>-1</sup> was previously reported at  
646 the study site without any difference between harvest and non-harvest treatments (Nielsen et  
647 al., 2024). The feasibility of using biomass from reed canary grass to offset fossil fuels would  
648 depend on the development of non-invasive harvesting techniques, the identification of viable  
649 and economically suitable uses for this biomass, and the establishment of markets and  
650 infrastructure for its processing.

651

## 652 **5. Conclusion**

653 We found that harvesting moderately fertilized RCG in the third production year did not  
654 increase net C emissions significantly in poorly drained fen peatlands compared to no  
655 management. Considering that the climate impact of rewetted sites under paludiculture  
656 depends on the fate of the harvested biomass, GHG emissions could be reduced elsewhere if  
657 this biomass is used to replace fossil fuels. When compared with emissions reported earlier  
658 for the second production year, the NECB was further reduced in the third production year as  
659 rewetting progressed. A main reason for no significant effect of management on NECB was  
660 the large differences between treatment replicates which could be partly related to different  
661 concentrations of nutrients in pore water and dynamics in WTD across the blocks.

662 Considering this field heterogeneity, results indicated that harvest of the biomass could  
663 potentially reduce net C fluxes at nutrient rich areas, while at relatively nutrient poor areas it  
664 seemed more advantageous to leave the grass without management. Paludiculture and  
665 management of RCG in rewetting fen peatlands, therefore, offers an alternative that could be

666 particularly beneficial in nutrient rich areas. We found that differences in annual NECB were  
667 highly influenced by  $R_{\text{eco}}$ , and that  $R_{\text{eco}}$  was best modelled by hourly data on RVI, WTD and  
668 Ts. The  $R_{\text{eco}}$  was underestimated when mean annual WTD was used instead of hourly values,  
669 indicating that temporal variability in WTD should be considered in establishing emission  
670 factors for rewetted fen peatlands. Differences in porewater nutrient concentrations were able  
671 to further improve prediction of  $R_{\text{eco}}$  based on a statistical model. As more nutrients could be  
672 related to higher CO<sub>2</sub> emissions, we suggest a feedback mechanism driving the  
673 mineralization, nutrient release, biomass production and peatland heterogeneity. Further  
674 research and the establishment of infrastructure and markets for harvested biomass would  
675 improve the prospects of paludiculture in rewetted peatlands.

676

#### 677 **Competing interests**

678 The authors declare that they have no conflict of interest.

679

#### 680 **Data availability**

681 Data on CO<sub>2</sub> and CH<sub>4</sub> fluxes as well as pore water nutrient concentrations will be available  
682 on Zenodo: <https://doi.org/10.5281/zenodo.14161801>

683

#### 684 **Author contributions**

685 PEL designed the experiment, methodology and directed data collection, AFR, JWMP, and  
686 PEL analyzed and visualized the data and wrote the original manuscript, all authors  
687 contributed in revising the manuscript.

688

689 **Acknowledgments** The authors would like to acknowledge the following people from the  
690 Agroecology Department at Aarhus University, Viborg: Michael Koppelgaard for his help in  
691 data collection and processing, Maarit Mäenpää for her help in the statistical analyses,  
692 Claudia Nielsen for her help in data processing, and Kirsten Kørup for her help in biomass  
693 harvesting.

694 **Funding sources**

695 This study was part of the INSURE project that received funding from the European Joint  
696 Programme EJP Soil under the European Union's Horizon 2020 research and innovation with  
697 grant agreement no. 862695. Co-funding was received from RePeat DK funded by the Danish  
698 Agricultural Agency.

699

700

701 **Appendix A**

702 Table A1. Biomass yields for each harvest event.

Harvest treatment	Block	Yield per harvest event (t DM ha <sup>-1</sup> )					Total
		20-May	16-jun	04-Aug	14-sep	11-Oct	
2	A	-	2.8	-	1.4	-	4.2
2	B	-	5.3	-	4.8	-	10.1
2	C	-	4.4	-	5.8	-	10.2
2	D	-	4.6	-	6.5	-	11.1
5	A	1.5	1.5	2.9	1.4	0.5	7.8
5	B	1.0	2.6	3.0	1.7	0.5	8.7
5	C	0.3	1.3	3.5	2.1	0.7	7.8
5	D	1.2	1.9	4.2	2.0	0.7	10.1

703

704 Table A2. Total N in harvested biomass per event

Harvest treatment	Block	Total N in biomass per harvest event (kg ha <sup>-1</sup> )					Total
		20-May	16-jun	04-Aug	14-sep	11-Oct	
2	A	-	62	-	31	-	93
2	B	-	104	-	91	-	195
2	C	-	99	-	116	-	215
2	D	-	91	-	113	-	204
5	A	49	38	56	40	21	204
5	B	34	61	65	52	20	233
5	C	13	35	93	74	31	245
5	D	41	47	83	59	27	258

705

706

707

708

709

710

711

712

713

714

715

716

717

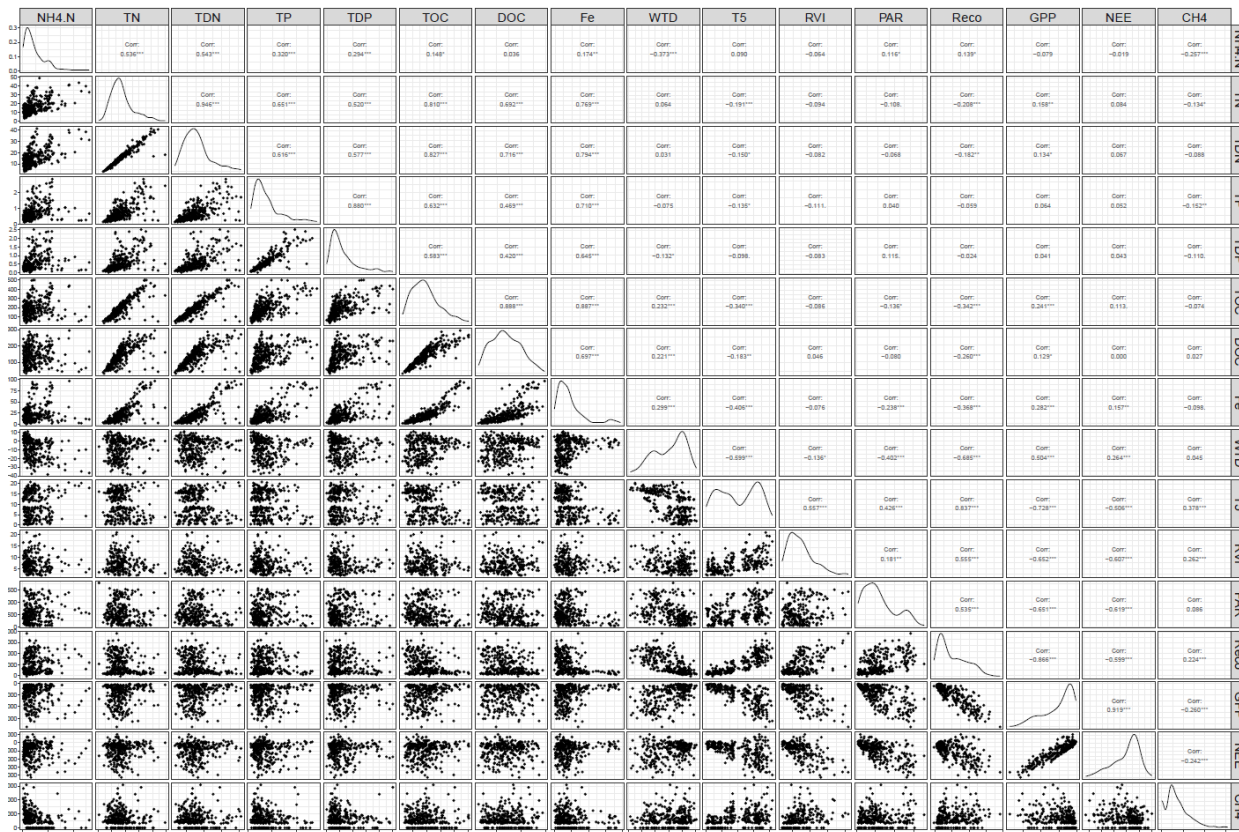
718 Table A3. Model evaluation for GPP model (model 1),  $R_{eco}$  models (models 2, 3, and 4), and  
 719  $CH_4$  model (model 5). Values are indexes of model performance for each block.

BL	T	Model 1			Model 2				Model 3				Model 4				Model 5		
		R <sup>2</sup>	NRMSE	NSE	R2	NRMSE	NSE	AICc	R2	NRMSE	NSE	AICc	R2	NRMSE	NSE	AICc	R <sup>2</sup>	NRMSE	NSE
A	0	0.9	31.1	0.9	1	21.4	1	980	1	19.4	1	1216	1	16.7	1	943	0.59	63.4	0.58
	2	0.9	24.2	0.9	0.9	39.2	0.8	1090	0.7	54.7	0.7	1424	0.9	34.8	0.9	1073	0.43	74.5	0.42
	5	0.9	33.9	0.9	0.7	53.5	0.7	1247	0.8	39.9	0.8	1481	0.8	42.5	0.8	1211	0.41	78.0	0.37
B	0	0.9	29.9	0.9	1	21.6	1	1029	0.9	26	0.9	1331	1	15.4	1	978	0.49	79.5	0.34
	2	1	19.3	1	0.7	53.3	0.7	1261	0.7	57.4	0.7	1570	0.7	50.7	0.7	1255	0.11	93.1	0.10
	5	0.9	24.4	0.9	0.8	40.7	0.8	1113	0.9	39	0.9	1389	0.9	38.3	0.9	1106	0.33	80.6	0.32
C	0	0.9	27.6	0.9	1	19.3	1	1109	0.9	27.7	0.9	1446	1	18.7	1	1106	0.17	93.9	0.08
	2	0.8	43.4	0.8	0.8	47.8	0.8	1175	0.7	53.8	0.7	1565	0.8	43.9	0.8	1163	0.03	156.4	-1.55
	5	0.9	30.6	0.9	0.8	39.6	0.8	1227	0.8	39.9	0.8	1519	0.8	39.6	0.8	1229	0.11	95.5	0.05
D	0	0.9	37.5	0.9	0.9	32.1	0.9	1030	0.9	36.4	0.9	1348	0.9	32.1	0.9	1032	0.49	72.7	0.45
	2	0.9	29.3	0.9	0.8	41.8	0.8	1229	0.8	43.3	0.8	1533	0.9	34.3	0.9	1198	0.50	70.5	0.48
	5	0.9	32.4	0.9	0.9	31.1	0.9	1153	0.8	40.1	0.8	1484	0.9	28.5	0.9	1142	0.55	72.5	0.45

720

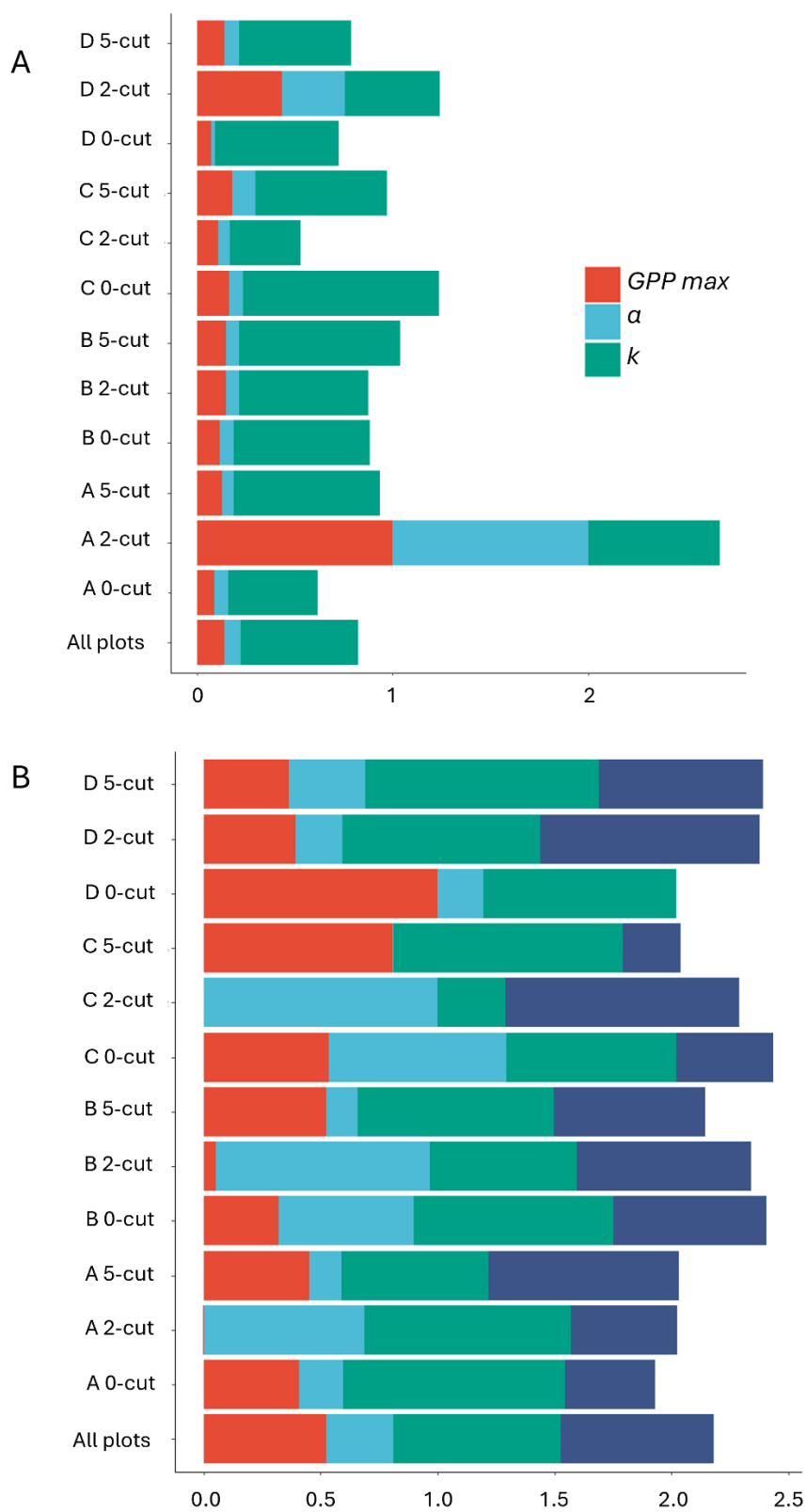
721 A, B, C, and D are the four block replicates (BL), 0, 2, and 5 are the three harvest treatments  
 722 (T) at each block. The four indexes of model evaluation are:  $R^2$ , normalized root mean square  
 723 of error (NRMSE), Nash-Sutcliffe efficiency (NSE), and corrected Akaike Information  
 724 Criteria (AICc).

725 Figure A1. Pearson's correlations of water chemistry parameters, Ecosystem respiration  
 726 ( $R_{eco}$ ), net ecosystem exchange (NEE), gross primary productivity (GPP), water table depth  
 727 (WTD), soil temperature at 5 cm depth (T5), ammonia (NH<sub>4</sub>.N), total nitrogen (TN), total  
 728 dissolved nitrogen (TDN), total phosphorus (TP), total dissolved phosphorus (TDP), total  
 729 organic carbon (TOC), and dissolved organic carbon (DOC). \* significant at  $p < 0.05$ , \*\*  
 730 significant at  $0.01 > p > 0.001$  \*\*\* significant at  $p < 0.001$



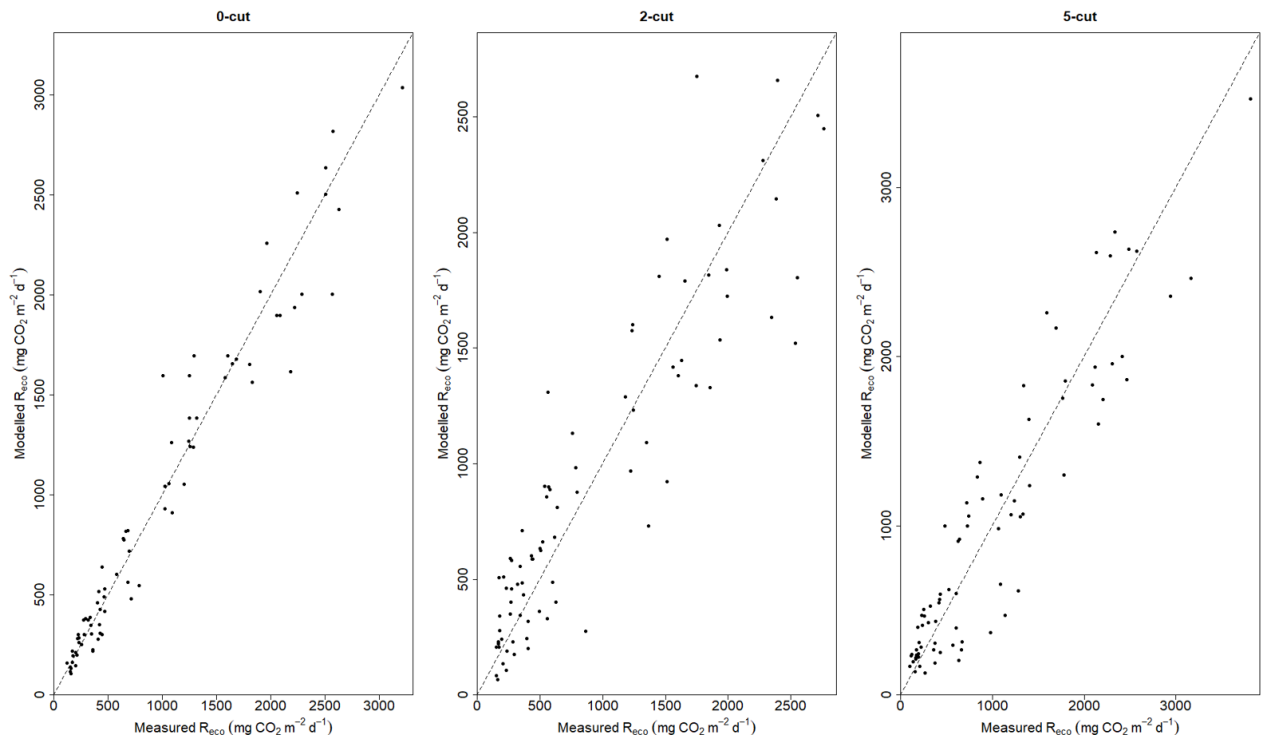
731  
 732  
 733  
 734  
 735  
 736  
 737  
 738  
 739  
 740  
 741  
 742  
 743

744 Figure A2. Variability of parameters fitted in  $R_{eco}$  model 4 (A) and the GPP model (B). Each bar  
 745 represents a plot, and the bottom bar corresponds to the model including all plots. Each color  
 746 represents a different parameter. Parameter values were normalized i.e. dividing them by the  
 747 maximum value.



749

750 Figure A3. 1:1 plots of measured vs. modelled Reco using model 4 for the three harvest  
751 treatments. All blocks are included each of the harvest treatments, N = 104.



752

753

754

755

756

757

758

759

760

761

762

763

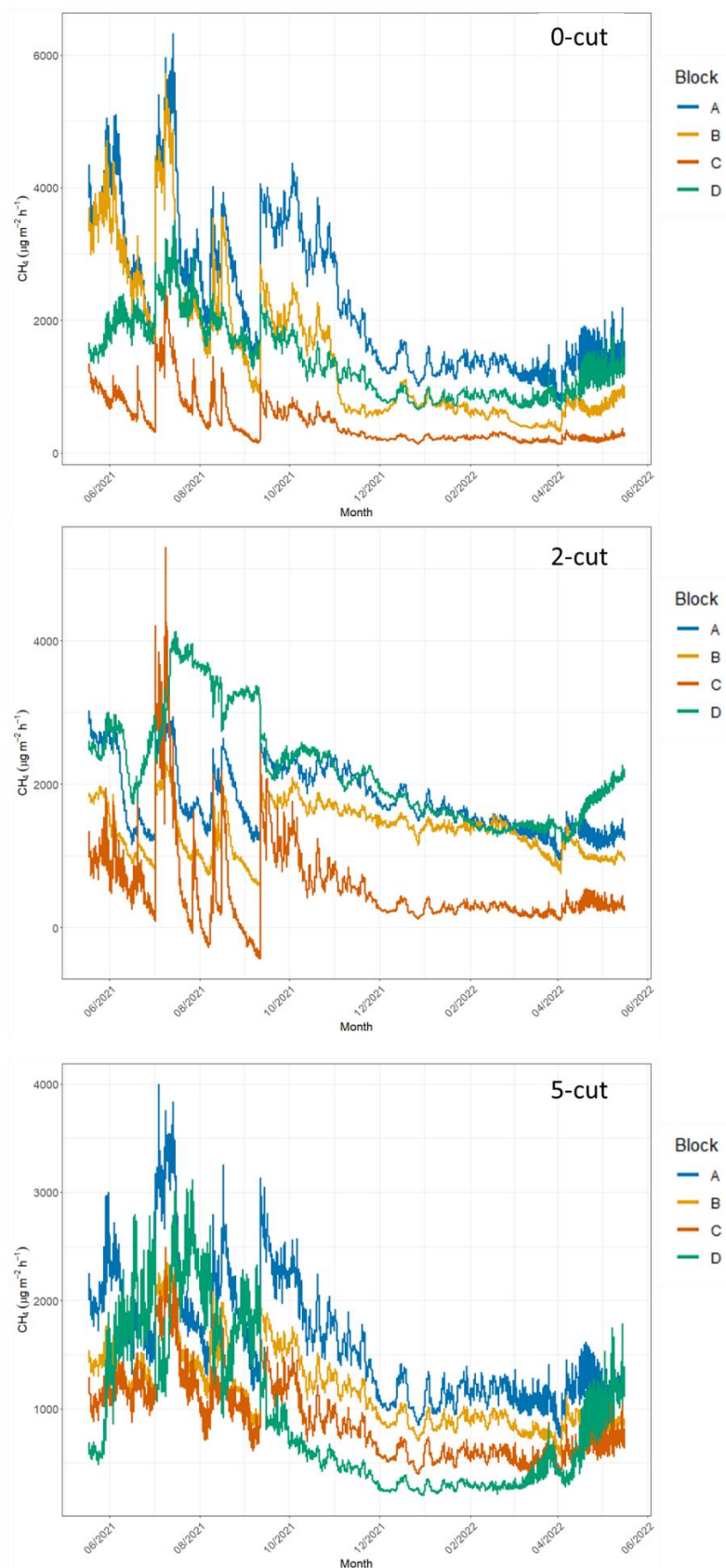
764

765

766

767

768 Figure A4. Time series of methane emissions from studied blocks (different line colors) and  
769 from the three harvest treatments (0-cut, 2-cut, and 5-cut). CH<sub>4</sub> emissions calculated only  
770 under 0% PAR conditions.



771

772 Table A4. Comparison of annual  $R_{eco}$  estimated with models 4, 2 and 3, which use hourly data  
 773 on Ts, WTD and RVI, model 4 using either mean annual WTD and Ts (M Model), and model  
 774 4 using mean annual WTD and hourly Ts (MH model), the latter two models including hourly  
 775 RVI data.

776

Block	Treatment	Model 4	Model 2	Model 3	M model	MH model
		t CO <sub>2</sub> -C ha <sup>-1</sup> yr <sup>-1</sup>				
A	0	15.4	14.9	15.4	12.2	14.8
B		18.6	18.4	18.9	14.4	17.7
C		26.2	26.1	25.6	21.6	25.8
D		29.4	29.4	31	25.9	29.4
Average ± SE		22.4 ± 3.3	22.2 ± 3.4	22.7 ± 3.5	18.5 ± 3.2	21.9 ± 3.4
A	2	14.9	14.5	15.1	12.3	13.9
B		23.6	23.4	23.6	20.5	22.4
C		26.4	25.7	26	24.1	24.4
D		23.7	22.7	23	18.7	21.4
Average ± SE		22.1 ± 2.5	21.6 ± 2.4	21.9 ± 2.4	18.9 ± 2.5	20.6 ± 2.3
A	5	20.6	18.6	19.3	17.4	18.6
B		21	20.8	20.5	17.0	19.7
C		23.7	23.6	23.4	19.8	23.4
D		24.3	22.9	23.4	17.9	22.6
Average ± SE		22.4 ± 0.9	21.5 ± 1.1	21.7 ± 1	18 ± 0.6	21.1 ± 1.1

777

778 Table A5. Total organic carbon (TOC), dissolved organic carbon (DOC), total nitrogen (TN),  
 779 total dissolved nitrogen (TDN), total phosphorus (TP), total dissolved phosphorus (TDP),  
 780 Turbidity (NTU), electrical conductivity (EC). If base model did not improve by adding the  
 781 water chemistry parameters, R<sup>2</sup> and RMSE are not shown.

782

Parameter	Reco models				GPP models			
	Base R <sup>2</sup>	Improved R <sup>2</sup>	Base RMSE	Improved RMSE	Base R <sup>2</sup>	Improved R <sup>2</sup>	Base RMSE	Improved RMSE
TOC	0.863	0.873	243	226	-	-	-	-
DOC	0.863	0.871	242	228	-	-	-	-
TN	0.863	0.870	244	229	-	-	-	-
TDN	0.864	0.876	242	224	-	-	-	-
NH <sub>4</sub>	-	-	-	-	-	-	-	-
TP	0.867	0.871	241	231	-	-	-	-
TDP	0.862	0.867	244	229	-	-	-	-
FE	0.863	0.878	242	225	-	-	-	-
pH	0.863	0.868	243	239	0.832	0.839	645	628
NTU	-	-	-	-	-	-	-	-
EC	-	-	-	-	0.832	0.839	643	624

783

784 Table A6. Model evaluation of  $R_{eco}$  and GPP models using all data pooled and modelling all  
785 blocks and harvest treatments all together.

$R_{eco}$ model	$R^2$	0.78
	NRMSE	46.6
	NSE	0.78
	AIC c	14223.49
GPP model	$R^2$	0.88
	NRMSE	34.2
	NSE	0.88

786 The four indexes of model evaluation are:  $R^2$ , normalized root mean square of error  
787 (NRMSE), Nash-Sutcliffe efficiency (NSE), and corrected Akaike Information Criteria.

788

789 Table A7. Carbon budget results obtained by using all data pooled and modelling all blocks  
 790 and harvest treatments all together to obtain models of  $R_{eco}$  and GPP.

Block	Treatment	Reco	GPP	NEE	Yield	CH <sub>4</sub>	NECB
		t CO <sub>2</sub> -C ha <sup>-1</sup>	t CO <sub>2</sub> -C ha <sup>-1</sup>	t CO <sub>2</sub> -C ha <sup>-1</sup>	t C ha <sup>-1</sup>	t CH <sub>4</sub> -C <sup>-1</sup>	t C ha <sup>-1</sup>
A	0-cut	21.1	-16.9	4.2	NA	0.15	4.3
B		18.8	-15.6	3.2	NA	0.10	3.3
C		21.6	-16.6	5.0	NA	0.03	5.1
D		23.0	-19.2	3.8	NA	0.09	3.9
Mean ± SE		21.1 ± 1.6	-17.1 ± 1.3	4.1 ± 0.7	NA	0.09 ± 0.02	4.2 ± 0.4
A	2-cut	21.9	-17.5	4.4	1.9	0.12	6.4
B		22.4	-19.3	3.1	4.5	0.09	7.7
C		23.7	-18.4	5.3	4.6	0.04	10.0
D		22.1	-16.6	5.5	5.0	0.14	10.7
Mean ± SE		22.6 ± 0.7	-17.9 ± 1	4.6 ± 1	4 ± 0.7	0.1 ± 0.02	8.7 ± 1
A	5-cut	23.9	-19.4	4.4	3.5	0.10	8.0
B		23.7	-20.8	2.9	3.9	0.08	6.8
C		25.7	-20.7	5.0	3.5	0.06	8.6
D		23.8	-20.3	3.5	4.5	0.06	8.0
Mean ± SE		24.3 ± 0.8	-20.3 ± 0.6	3.9 ± 0.8	3.8 ± 0.2	0.08 ± 0.01	7.9 ± 0.4

791

792  $R_{eco}$  is ecosystem respiration, GPP is gross primary productivity, NEE is net ecosystem  
 793 exchange, and NECB is the net ecosystem carbon balance (NEE + yield + CH<sub>4</sub>).

794

795 **References**

- 796 Abdalla, M., Hastings, A., Truu, J., Espenberg, M., Mander, Ü., and Smith, P.: Emissions of  
797 methane from northern peatlands: a review of management impacts and implications for  
798 future management options, *Ecology and Evolution*, 6(19), 7080-7102, 2016.
- 799 AminiTabrizi, R., Dontsova, K., Grachet, N. G., and Tfaily, M. M.: Elevated temperatures  
800 drive abiotic and biotic degradation of organic matter in a peat bog under oxic conditions,  
801 *Science of the Total Environment*, 804, 150045, 2022.
- 802 Andersen, R., Farrell, C., Graf, M., Muller, F., Calvar, E., Frankard, P., Caporn, S and  
803 Anderson, P.: An overview of the progress and challenges of peatland restoration in Western  
804 Europe, *Restoration Ecology*, 25(2), 271-282, 2017.
- 805 Arsenault, J., Talbot, J., and Moore, T. R.: Environmental controls of C, N and P  
806 biogeochemistry in peatland pools, *Science of the Total Environment*, 631, 714-722, 2018.
- 807 Arsenault, J., Talbot, J., Moore, T. R., Beauvais, M. P., Franssen, J., and Roulet, N. T. The  
808 spatial heterogeneity of vegetation, hydrology and water chemistry in a peatland with open-  
809 water pools, *Ecosystems*, 22, 1352-1367, 2019.
- 810 Best, E. K.: An automated method for determining nitrate nitrogen in soil  
811 extracts, *Queensland Journal of Agricultural and Animal Sciences*, 33, 161-166, 1976.
- 812 Bianchi, A., Larmola, T., Kekkonen, H., Saarnio, S., and Lång, K: Review of greenhouse gas  
813 emissions from rewetted agricultural soils, *Wetlands*, 41, 1-7, 2021.
- 814 Bockermann, C., Eickenscheidt, T., and Drösler, M.: Adaptation of fen peatlands to climate  
815 change: rewetting and management shift can reduce greenhouse gas emissions and offset  
816 climate warming effects, *Biogeochemistry*, 167 (4), 563-588, 2024.
- 817 Bourbonniere, R. A.: Review of water chemistry research in natural and disturbed  
818 peatlands, *Canadian water resources journal*, 34(4), 393-414, 2009.
- 819 Bridgham, S. D., and Richardson, C. J.: Hydrology and nutrient gradients in North Carolina  
820 peatlands, *Wetlands*, 13, 207-218, 1993.
- 821 Cabezas, A., Gelbrecht, J., Zwirnmann, E., Barth, M., and Zak, D.: Effects of degree of peat  
822 decomposition, loading rate and temperature on dissolved nitrogen turnover in rewetted  
823 fens, *Soil Biology and Biochemistry*, 48, 182-191, 2012.
- 824 Cabezas, A., Gelbrecht, J., and Zak, D.: The effect of rewetting drained fens with nitrate-  
825 polluted water on dissolved organic carbon and phosphorus release, *Ecological  
826 engineering*, 53, 79-88, 2013.
- 827 Chroňáková, A., Bárta, J., Kaštovská, E., Urbanová, Z., and Pícek, T.: Spatial heterogeneity  
828 of belowground microbial communities linked to peatland microhabitats with different plant  
829 dominants, *FEMS Microbiology Ecology*, 95(9), fiz130,  
830 <https://doi.org/10.1093/femsec/fiz130>, 2019.
- 831 Croke, W. M., and Simpson, W. E.: Determination of ammonium in Kjeldahl digests of  
832 crops by an automated procedure, *Journal of the Science of Food and Agriculture*, 22(1), 9-  
833 10., 1971.

834 Dansk Standard: DS 291. Water Analyses – orthophosphate-phosphorus. Photometric  
835 method, 2004.

836 Darusman, T., Murdiyarso, D., Impron, and Anas, I.: Effect of rewetting degraded peatlands  
837 on carbon fluxes: a meta-analysis, *Mitigation and Adaptation Strategies for Global*  
838 *Change*, 28(3), 10, 2023.

839 de Jong, M., van Hal, O., Pijlman, J., van Eekeren, N., and Junginger, M.: Paludiculture as  
840 paludifuture on Dutch peatlands: An environmental and economic analysis of *Typha*  
841 cultivation and insulation production, *Science of the Total Environment*, 792, 148161, 2021.

842 Dragoni, F., Giannini, V., Ragaglini, G., Bonari, E., and Silvestri, N.: Effect of harvest time  
843 and frequency on biomass quality and biomethane potential of common reed (*Phragmites*  
844 *australis*) under paludiculture conditions, *BioEnergy research*, 10, 1066-1078, 2017.

845 Elsgaard, L., Görres, C. M., Hoffmann, C. C., Blicher-Mathiesen, G., Schelde, K., and  
846 Petersen, S. O.: Net ecosystem exchange of CO<sub>2</sub> and carbon balance for eight temperate  
847 organic soils under agricultural management, *Agriculture, ecosystems and environment*, 162,  
848 52-67, 2012.

849 Emsens, W. J., van Diggelen, R., Aggenbach, C. J., Cajthaml, T., Frouz, J., Klimkowska, A.,  
850 Kotowski, W., Kozub, L., Liczner, Y., Seeber, E., Silvennoinen, H., Tanneberger, F., Vicena,  
851 J., Wilk, M., and Verbruggen, E.: Recovery of fen peatland microbiomes and predicted  
852 functional profiles after rewetting, *The ISME journal*, 14(7), 1701-1712, 2020.

853 Erb, K. H., Kastner, T., Plutzer, C., Bais, A. L. S., Carvalhais, N., Fetzel, T., Gingrich, S.,  
854 Haberl, H., Lauk, C., Niedertscheider, M., Pongratz, J., Thurner, M., and Luysaert, S.:  
855 Unexpectedly large impact of forest management and grazing on global vegetation  
856 biomass, *Nature*, 553(7686), 73-76, <https://doi.org/10.1038/nature25138>, 2018.

857 Evans, C. D., Peacock, M., Baird, A. J., Artz, R. R. E., Burden, A., Callaghan, N., ... and  
858 Morrison, R.: Overriding water table control on managed peatland greenhouse gas  
859 emissions, *Nature*, 593(7860), 548-552, 2021.

860 Forster, P., Storelvmo, T., Armour, K., Collins, W., Dufresne, J.-L., Frame, D., Lunt, D. J.,  
861 Mauritsen, T., Palmer, M. D., Watanabe, M., Wild, M., and Zhang, H. (2021). The Earth's  
862 energy budget, climate feedbacks, and climate sensitivity. In V. Masson-Delmotte, P. Zhai, A.  
863 Pirani, S. L. Connors, C. Péan, S. Berger, N. Caud, Y. Chen, L. Goldfarb, M. I. Gomis, M.  
864 Huang, K. Leitzell, E. Lonnoy, J. B. R. Matthews, T. K. Maycock, T. Waterfield, O. Yelekçi,  
865 R. Yu, and B. Zhou (Eds.): *Climate change 2021: The physical science basis. Contribution of*  
866 *Working Group I to the Sixth Assessment Report of the Intergovernmental Panel on Climate*  
867 *Change*, Cambridge University Press, (pp. 923–1054),  
868 <https://doi.org/10.1017/9781009157896.009>, 2021.

869 Geurts, J. J., Oehmke, C., Lambertini, C., Eller, F., Sorrell, B. K., Mandiola, S. R., Grootjans,  
870 A.P., Brix, H., Wichtmann, W., Lamers, L.P., and Fritz, C.: Nutrient removal potential and  
871 biomass production by *Phragmites australis* and *Typha latifolia* on European rewetted peat  
872 and mineral soils, *Science of the Total Environment*, 747, 141102, 2020.

873 Giannini, V., Silvestri, N., Dragoni, F., Pistocchi, C., Sabbatini, T., and Bonari, E.: Growth  
874 and nutrient uptake of perennial crops in a paludicultural approach in a drained  
875 Mediterranean peatland, *Ecological engineering*, 103, 478-487, 2017.

876 Görres, C. M., Kutzbach, L., and Elsgaard, L.: Comparative modeling of annual CO<sub>2</sub> flux of  
877 temperate peat soils under permanent grassland management, *Agriculture, ecosystems and  
878 environment*, 186, 64-76, 2014.

879 Griffiths, N. A., Sebestyen, S. D., and Oleheiser, K. C.: Variation in peatland porewater  
880 chemistry over time and space along a bog to fen gradient, *Science of the total  
881 environment*, 697, 134152, 2019.

882 Haapalehto, T., Kotiaho, J. S., Matilainen, R., and Tahvanainen, T.: The effects of long-term  
883 drainage and subsequent restoration on water table level and pore water chemistry in boreal  
884 peatlands, *Journal of Hydrology*, 519, 1493-1505, 2014.

885 Hartung, C., Andrade, D., Dandikas, V., Eickenscheidt, T., Drösler, M., Zollfrank, C., and  
886 Heuwinkel, H.: Suitability of paludiculture biomass as biogas substrate– biogas yield and  
887 long-term effects on anaerobic digestion, *Renewable energy*, 159, 64-71, 2020.

888 Hemes, K. S., Chamberlain, S. D., Eichelmann, E., Anthony, T., Valach, A., Kasak, K., Szutu,  
889 D., Verfaillie, J., Silver, W.L. and Baldocchi, D.D.: Assessing the carbon and climate benefit  
890 of restoring degraded agricultural peat soils to managed wetlands, *Agricultural and Forest  
891 Meteorology*, 268, 202-214, 2019.

892 Jurasinski G, Koebisch F, Guenther A, Beetz S.: `_flux`: Flux Rate Calculation from Dynamic  
893 Closed Chamber Measurements. R package version 0.3-0.1, <[https://CRAN.R-  
894 project.org/package=flux](https://CRAN.R-project.org/package=flux)>, 2022.

895 Juszczak, R., Humphreys, E., Acosta, M., Michalak-Galczewska, M., Kayzer, D., and  
896 Olejnik, J.: Ecosystem respiration in a heterogeneous temperate peatland and its sensitivity to  
897 peat temperature and water table depth, *Plant and Soil*, 366, 505-520., 2013.

898 Kandel, T. P., Sutaryo, S., Møller, H. B., Jørgensen, U., and Lærke, P. E.: Chemical  
899 composition and methane yield of reed canary grass as influenced by harvesting time and  
900 harvest frequency, *Bioresource technology*, 130, 659-666, 2013.

901 Kandel, T. P., Elsgaard, L., and Lærke, P. E.: Annual balances and extended seasonal  
902 modelling of carbon fluxes from a temperate fen cropped to *festulolium* and tall fescue under  
903 two-cut and three-cut harvesting regimes, *GCB Bioenergy*, 9(12), 1690-1706, 2017.

904 Kandel, T. P., Karki, S., Elsgaard, L., and Lærke, P. E.: Fertilizer-induced fluxes dominate  
905 annual N<sub>2</sub>O emissions from a nitrogen-rich temperate fen rewetted for  
906 paludiculture, *Nutrient Cycling in Agroecosystems*, 115, 57-67, 2019.

907 Karki, S., Elsgaard, L., Audet, J., and Lærke, P. E.: Mitigation of greenhouse gas emissions  
908 from reed canary grass in paludiculture: effect of groundwater level, *Plant and Soil*, 383(1),  
909 217-230, 2014.

910 Karimi, S., Hasselquist, E. M., Salimi, S., Järveoja, J., and Laudon, H.: Rewetting impact on  
911 the hydrological function of a drained peatland in the boreal landscape, *Journal of  
912 Hydrology*, 641, 131729, 2024.

913 Kreyling, J., Tanneberger, F., Jansen, F., Van Der Linden, S., Aggenbach, C., Blüml, V.,  
914 Couwenberg, J., Emsens, W.J., Joosten, H., Klimkowska, Kotowski, W., Kozub, L., Lennartz,  
915 B., Liczner, Y., Liu, H., Michaelis, D., Oehmke, C., Parakenings, K., Pleyl, E., Poyda, A.,  
916 Raabe, S., Röhl, M., Rücker, K., Schneider, A., Schrautzer, J., Schröder, C., Schug, F., Seeber,  
917 E., Thiel, F., Thiele, S., Tiemeyer, B., Timmermann, T., Urich, T., van Diggelen, R., Vegelin,  
918 K., Verbruggen, E., Wilmking, M., Wrage-Mönnig, N., Wolejko, L., Zak, D., and Jurasinski,  
919 G.: Rewetting does not return drained fen peatlands to their old selves, *Nature*  
920 *communications*, 12(1), 5693, 2021.

921 Koch, J., Elsgaard, L., Greve, M. H., Gyldenkerne, S., Hermansen, C., Levin, G., Wu, S., and  
922 Stisen, S.: Water table driven greenhouse gas emission estimate guides peatland restoration at  
923 national scale, *Biogeosciences Discussions*, 2023, 1-28, 2023.

924 Kou, D., Virtanen, T., Treat, C. C., Tuovinen, J. P., Räsänen, A., Juutinen, S., Mikola, J.,  
925 Aurela, M., Heiskanen, L., Heikkilä, M., Weckström, J., Juselius, T., Piilo, S. R., Deng, J.,  
926 Zhang, Y., Chaudhary, N., Huang, C., Välianta, M., Biasi, C., Liu, X., Guo, M., Zhuang, Q.,  
927 Korhola, A., Shurpali, N. J.: Peatland heterogeneity impacts on regional carbon flux and its  
928 radiative effect within a boreal landscape, *Journal of Geophysical Research:*  
929 *Biogeosciences*, 127(9), e2021JG006774. <https://doi.org/10.1029/2021JG006774>, 2022.

930 Lafleur, P. M., Moore, T. R., Roulet, N. T., and Frolking, S.: Ecosystem respiration in a cool  
931 temperate bog depends on peat temperature but not water table, *Ecosystems*, 8, 619-629,  
932 2005.

933 Larmola, T., Bubier, J. L., Kobyljanec, C., Basiliko, N., Juutinen, S., Humphreys, E., Preston,  
934 M., and Moore, T. R.: Vegetation feedbacks of nutrient addition lead to a weaker carbon sink  
935 in an ombrotrophic bog, *Global Change Biology*, 19(12), 3729-3739, 2013.

936 Leifeld, J., and Menichetti, L.: The underappreciated potential of peatlands in global climate  
937 change mitigation strategies, *Nature communications*, 9(1), 1071, 2018.

938 Leifeld, J., Wüst-Galley, C., and Page, S.: Intact and managed peatland soils as a source and  
939 sink of GHGs from 1850 to 2100, *Nature Climate Change*, 9(12), 945-947, 2019.

940 Liu, H., Zak, D., Rezanezhad, F., and Lennartz, B.: Soil degradation determines release of  
941 nitrous oxide and dissolved organic carbon from peatlands, *Environmental Research*  
942 *Letters*, 14(9), 094009, 2019.

943 Liu, W., Fritz, C., Weideveld, S. T., Aben, R. C., Van Den Berg, M., and Velthuis, M.: Annual  
944 CO<sub>2</sub> budget estimation from chamber-based flux measurements on intensively drained peat  
945 meadows: Effect of gap-filling strategies, *Frontiers in Environmental Science*, 10, 803746.,  
946 2022.

947 Loisel, J., and Gallego-Sala, A.: Ecological resilience of restored peatlands to climate  
948 change, *Communications Earth & Environment*, 3(1), 208, 2022.

949 Lundin, L., Nilsson, T., Jordan, S., Lode, E., and Strömberg, M.: Impacts of rewetting on  
950 peat, hydrology and water chemical composition over 15 years in two finished peat extraction  
951 areas in Sweden, *Wetlands ecology and management*, 25, 405-419, 2017.

952 Lång, K., Honkanen, H., Heikkinen, J., Saarnio, S., Larmola, T., and Kekkonen, H.: Impact of  
953 crop type on the greenhouse gas (GHG) emissions of a rewetted cultivated peatland, *Soil*,  
954 10(2), 827-841, 2024.

955 Malinowski, R., Groom, G., Schwanghart, W., and Heckrath, G.: Detection and delineation of  
956 localized flooding from WorldView-2 multispectral data. *Remote sensing*, 7(11), 14853-  
957 14875, 2015.

958 Mashhadi, S. R., Grombacher, D., Zak, D., Lærke, P. E., Andersen, H. E., Hoffmann, C. C.,  
959 and Petersen, R. J.: Borehole nuclear magnetic resonance as a promising 3D mapping tool in  
960 peatland studies, *Geoderma*, 443, 116814, 2024.

961 Nielsen, C. K., Stødkilde, L., Jørgensen, U., and Lærke, P. E.: Effects of harvest and  
962 fertilization frequency on protein yield and extractability from flood-tolerant perennial  
963 grasses cultivated on a fen peatland, *Frontiers in Environmental Science*, 9, 619258, 2021.

964 Nielsen, C. K., Stødkilde, L., Jørgensen, U., and Lærke, P. E.: Ratio vegetation indices have  
965 the potential to predict extractable protein yields in green protein paludiculture, *Mires and*  
966 *Peat*, (29), 2023a.

967 Nielsen, C. K., Elsgaard, L., Jørgensen, U., and Lærke, P. E.: Soil greenhouse gas emissions  
968 from drained and rewetted agricultural bare peat mesocosms are linked to  
969 geochemistry, *Science of the Total Environment*, 896, 165083, 2023b.

970 Nielsen, C. K., Liu, W., Koppelgaard, M., and Lærke, P. E.: To Harvest or not to Harvest:  
971 Management Intensity did not Affect Greenhouse Gas Balances of *Phalaris Arundinacea*  
972 Paludiculture, *Wetlands*, 44(6), 79, 2024.

973 Page, S. E., and Baird, A. J.: Peatlands and global change: response and resilience, *Annual*  
974 *Review of Environment and Resources*, 41, 35-57, 2016.

975 Piilo, S. R., Korhola, A., Heiskanen, L., Tuovinen, J. P., Aurela, M., Juutinen, S., Marttila, H.,  
976 Saari, M., Tuittila, E. S., Turunen, J., Väiliranta, M. M.: Spatially varying peatland initiation,  
977 Holocene development, carbon accumulation patterns and radiative forcing within a subarctic  
978 fen, *Quaternary Science Reviews*, 248, 106596, 2020.

979 Purre, A. H., Penttilä, T., Ojanen, P., Minkkinen, K., Aurela, M., Lohila, A., and Ilomets, M.:  
980 Carbon dioxide fluxes and vegetation structure in rewetted and pristine peatlands in Finland  
981 and Estonia, *Boreal Environment Research*, 24, 1-6, 2019.

982 Putkinen, A., Tuittila, E. S., Siljanen, H. M., Bodrossy, L., and Fritze, H.: Recovery of  
983 methane turnover and the associated microbial communities in restored cutover peatlands is  
984 strongly linked with increasing *Sphagnum* abundance, *Soil Biology and Biochemistry*, 116,  
985 110-119, 2018.

986 R Core Team: R: A Language and Environment for Statistical Computing, R Foundation for  
987 Statistical Computing, Vienna, Austria, <https://www.R-project.org/>, 2023.

988 Ren, L., Eller, F., Lambertini, C., Guo, W. Y., Brix, H., and Sorrell, B. K.: Assessing nutrient  
989 responses and biomass quality for selection of appropriate paludiculture crops, *Science of the*  
990 *Total Environment*, 664, 1150-1161, 2019.

- 991 Scharlemann, J. P., Tanner, E. V., Hiederer, R., and Kapos, V.: Global soil carbon:  
 992 understanding and managing the largest terrestrial carbon pool, *Carbon management*, 5(1),  
 993 81-91, 2014.
- 994 Silvola, J., Alm, J., Ahlholm, U., Nykanen, H., and Martikainen, P. J.: CO<sub>2</sub> fluxes from peat  
 995 in boreal mires under varying temperature and moisture conditions, *Journal of ecology*, 219-  
 996 228, 1996.
- 997 Rigney, C., Wilson, D., Renou-Wilson, F., Müller, C., Moser, G., and Byrne, K. A.:  
 998 Greenhouse gas emissions from two rewetted peatlands previously managed for forestry.  
 999 *Mires and Peat*, 21, 1-23, 2018.
- 1000 Song, Y., Cheng, X., Song, C., Li, M., Gao, S., Liu, Z., Gao, J., and Wang, X.: Soil CO<sub>2</sub> and  
 1001 N<sub>2</sub>O emissions and microbial abundances altered by temperature rise and nitrogen addition in  
 1002 active-layer soils of permafrost peatland, *Frontiers in Microbiology*, 13, 1093487, 2022.
- 1003 Tanneberger, F., Schröder, C., Hohlbein, M., Lenschow, U., Permien, T., Wichmann, S., and  
 1004 Wichtmann, W.: Climate change mitigation through land use on rewetted peatlands—cross-  
 1005 sectoral spatial planning for paludiculture in Northeast Germany, *Wetlands*, 40(6), 2309-  
 1006 2320, 2020.
- 1007 Thers, H., Knudsen, M. T., and Lærke, P. E.: Comparison of GHG emissions from annual  
 1008 crops in rotation on drained temperate agricultural peatland with production of reed canary  
 1009 grass in paludiculture using an LCA approach, *Heliyon*, 9(6), 2023.
- 1010 Tiemeyer, B., Freibauer, A., Borraz, E. A., Augustin, J., Bechtold, M., Beetz, S., Beyer, C.,  
 1011 Ebli, M., Eickenscheidt, T., Fiedler, S., Förster, C., Gensior, A., Giebels, M., Glatzel, S.,  
 1012 Heinichen, J., Hoffmann, M., Höper, H., Jurasinski, G., Laggner, A., Leiber-Sauheitl, K.,  
 1013 Peichl-Brak, M., and Drösler, M.: A new methodology for organic soils in national  
 1014 greenhouse gas inventories: Data synthesis, derivation and application, *Ecological*  
 1015 *Indicators*, 109, 105838, 2020.
- 1016 Urbanová, Z., and Bárta, J.: Recovery of methanogenic community and its activity in long-  
 1017 term drained peatlands after rewetting, *Ecological engineering*, 150, 105852, 2020.
- 1018 Vroom, R. J., Xie, F., Geurts, J. J., Chojnowska, A., Smolders, A. J., Lamers, L. P., and Fritz,  
 1019 C.: *Typha latifolia* paludiculture effectively improves water quality and reduces greenhouse  
 1020 gas emissions in rewetted peatlands, *Ecological engineering*, 124, 88-98, 2018.
- 1021 Wilson, D., Blain, D., Couwenberg, J., Evans, C. D., Murdiyarso, D., Page, S., Renou-  
 1022 Wilson, F., Rieley, J. O., Sirin, A., Strack, M., and Tuittila, E. S.: Greenhouse gas emission  
 1023 factors associated with rewetting of organic soils, *Mires and Peat*, 17, 1-28, 2016.
- 1024 Wood, M. E., Macrae, M. L., Strack, M., Price, J. S., Osko, T. J., and Petrone, R. M., Spatial  
 1025 variation in nutrient dynamics among five different peatland types in the Alberta oil sands  
 1026 region, *Ecohydrology*, 9(4), 688-699, 2016.
- 1027 Yu, Z., Loisel, J., Brosseau, D. P., Beilman, D. W., and Hunt, S. J.: Global peatland dynamics  
 1028 since the Last Glacial Maximum, *Geophysical research letters*, 37(13), 2010.

- 1029 Zak, D., Roth, C., Unger, V., Goldhammer, T., Fenner, N., Freeman, C., and Jurasinski, G.:  
1030 Unraveling the importance of polyphenols for microbial carbon mineralization in rewetted  
1031 riparian peatlands, *Frontiers in Environmental Science*, 7, 147, 2019.
- 1032 Zambrano-Bigiarini, M.: hydroGOF: Goodness-of-fit functions for comparison of simulated  
1033 and observed hydrological time series, R package version 0.4-0,  
1034 <https://github.com/hzambran/hydroGOF>, DOI:10.5281/zenodo.839854, 2020.
- 1035 Zhong, Y., Jiang, M., and Middleton, B. A.: Effects of water level alteration on carbon  
1036 cycling in peatlands, *Ecosystem Health and Sustainability*, 6(1), 1806113, 2020.
- 1037 Ziegler, R.: Paludiculture as a critical sustainability innovation mission, *Research*  
1038 *Policy*, 49(5), 103979, 2020.